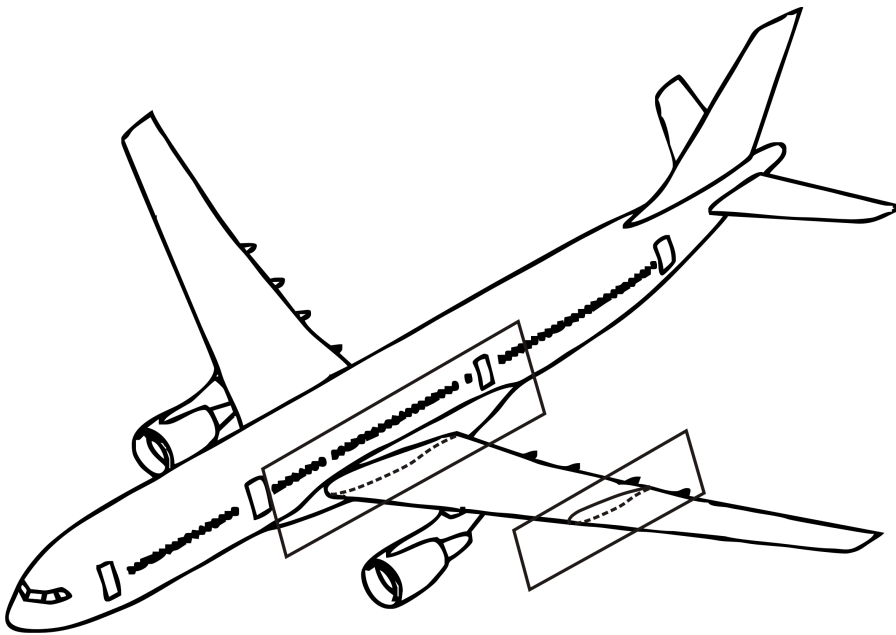


## 7 Wing Design

During the preliminary sizing, the wing was merely described in terms of the *wing area*  $S_W$  and the *wing aspect ratio*  $A_W$ . When designing the wing, other wing parameters are determined. This involves the definition of the *wing section* and the *planform*.

### 7.1 Wing Parameters



**Fig. 7.1**  
Definition of the wing sections

Wing sections are positioned parallel to the plane of symmetry of the aircraft (**Fig. 7.1**). A wing section is produced by scaling up an airfoil section. The *airfoil section* is described by the section coordinates of the top of the section  $y_u = f(x)$  and the bottom of the section  $y_l = f(x)$  with  $0 \leq x \leq 1$ . Sections can also be described by the *thickness distribution*  $t = f(x)$  combined with the *camber*  $y_c = f(x)$ . **Fig. 7.2** contains additional parameters for describing the section geometry:

Chord	$c$
Thickness	$t$
Camber	$(y_c)_{max} / c$
Position of maximum thickness	$x_t$
Position of maximum camber	$x_{(y_c)_{max}}$
Leading edge radius	$r$
Trailing edge angle	$\Phi_{TE}$

Fig. 7.2 also defines the following:

Chord line

(Mean) camber line

Leading edge LE

Trailing edge TE

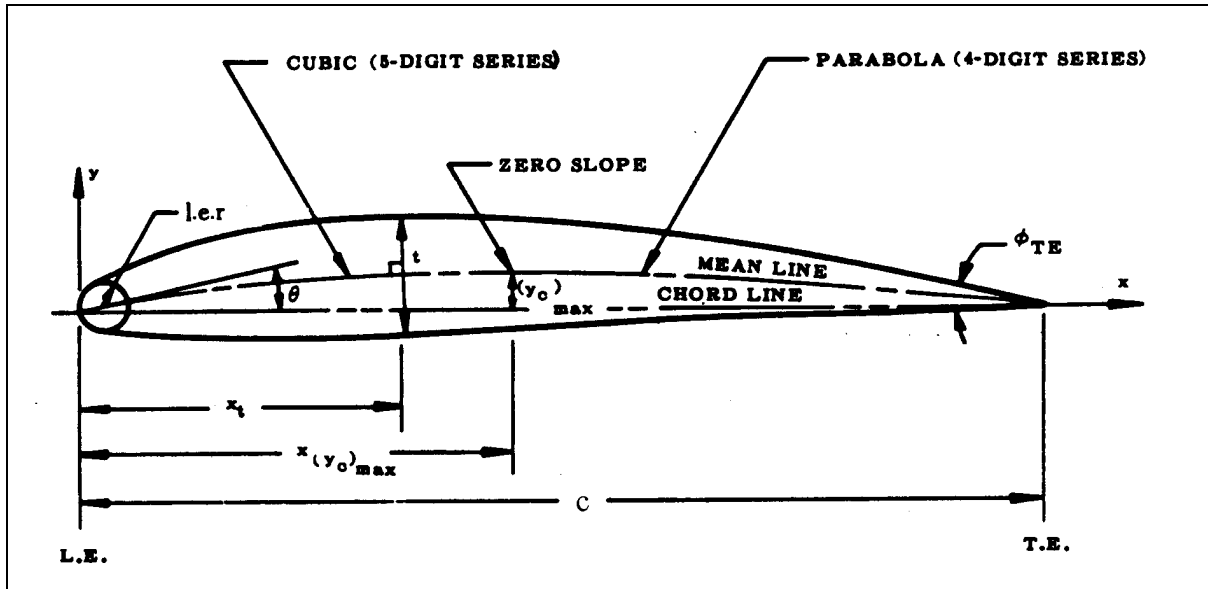


Fig. 7.2: Airfoil geometry (DATCOM 1978)

For simplicity of production, planforms with a curved leading and trailing edge are rare. Wings can therefore very often be described as double tapered wings (Fig. 7.3). The simple tapered wing and the rectangular wing can be seen as special versions of the double tapered wing. The *sweep angle*  $\phi$  depends on the % line<sup>1</sup> on which it is measured. Normally the sweep angle of the leading edge  $\phi_{LE}$ , trailing edge  $\phi_{TE}$ , 25% line  $\phi_{25}$  (quarter chord sweep) and 50% line  $\phi_{50}$  are stated.

The point where the inner and outer taper meet is called the *kink*. At this *kink*, the local chord is called  $c_k$ . In contrast to the chord at the *wing tip*  $c_t$  a chord does not actually exist on the *wing root*  $c_r$ , but is only created by graphically extending the leading and trailing edge as far as the plane of symmetry – and therefore into the fuselage. The *mean aerodynamic chord*  $c_{MAC}$  is the chord of an equivalent untwisted, unswept rectangular wing that achieves the same lift and the same pitching moment as this wing. The *aerodynamic center*, *AC* lies on the mean aerodynamic chord. The aerodynamic center is characterized by the following feature: if

<sup>1</sup> n% point: point on a local chord that is located n% of the local chord behind the leading edge.

n% line: line formed by the geometric locations of the n% points of the chords.

Note: In this case “n%” is replaced by a percentage (e.g. 25%) or another figure symbolizing the percentage (e.g. c/4).

we take an axis that is perpendicular to the plane of symmetry of the aircraft and passes through the aerodynamic center, the pitching moment of the wing about this axis is constant and independent of the lift. The position of the aerodynamic center  $X_{AC}$  on a rectangular wing with a thin symmetrical section is  $0.25 \cdot c_{MAC}$ . **Torenbeek 1988** (Fig. E10) contains details of the position of the aerodynamic center on simple tapered wings.

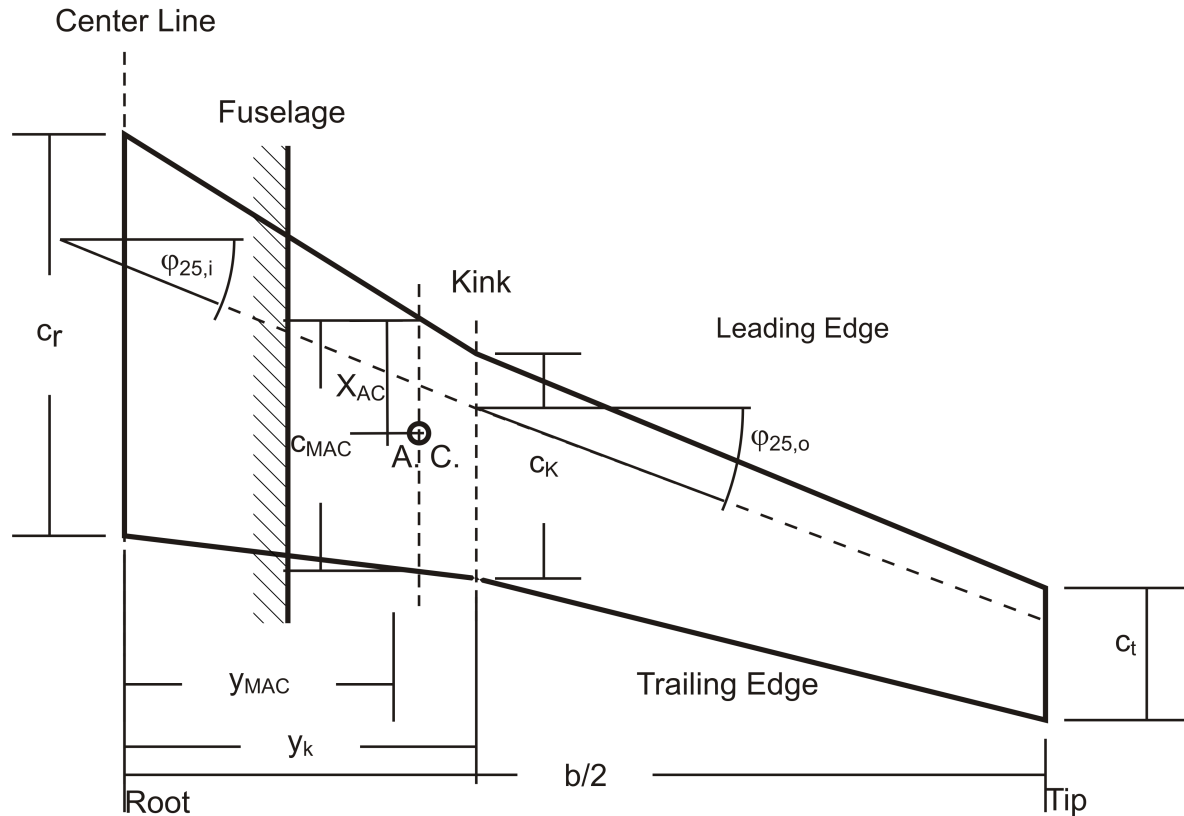


**Fig. 7.3** Geometry of the double tapered wing

Wing area  $S_w$  does not just include the visible part of the wing. The wing area also includes the area of the inner taper in the fuselage. The exact size of the wing area is not really important. All that is needed for the calculations is a standard reference wing area  $S_{ref}$ . Why is this? Let's take a look at the calculation for lift in cruise flight, for example:  $m \cdot g = L = 1/2 \rho v^2 \cdot C_L \cdot S_{ref}$ . If  $S_{ref}$  is changed, only the lift coefficient  $C_L$  changes (by definition). For this reason, aircraft manufacturers often use their own in-house definition of the (reference) wing area. **Fig. 7.4** and **Fig. 7.5** show such differing definitions of the wing area.

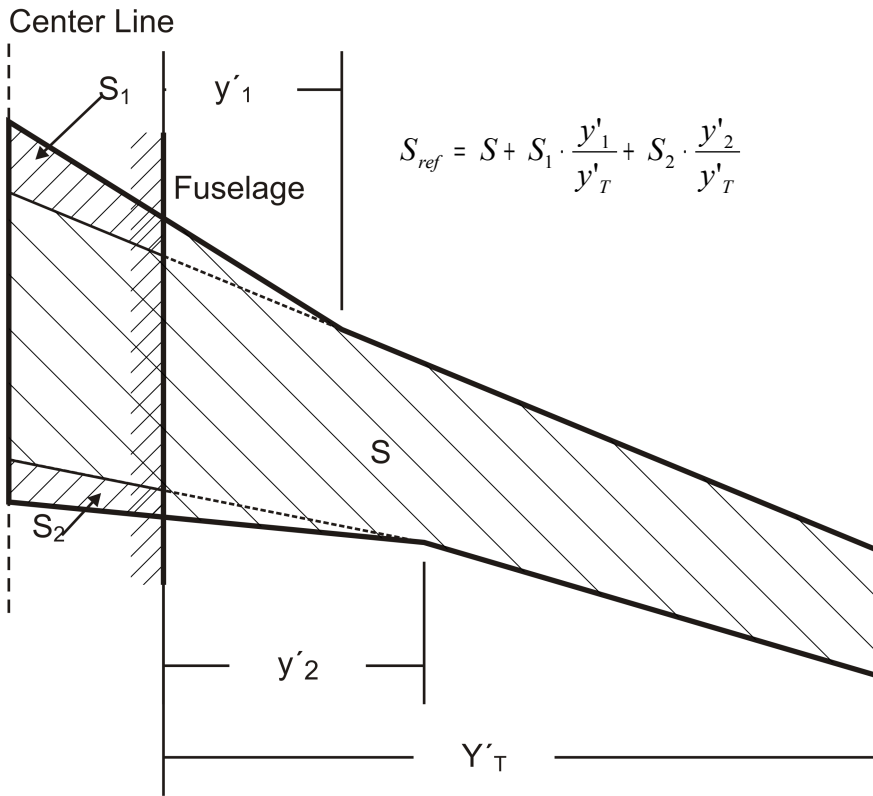
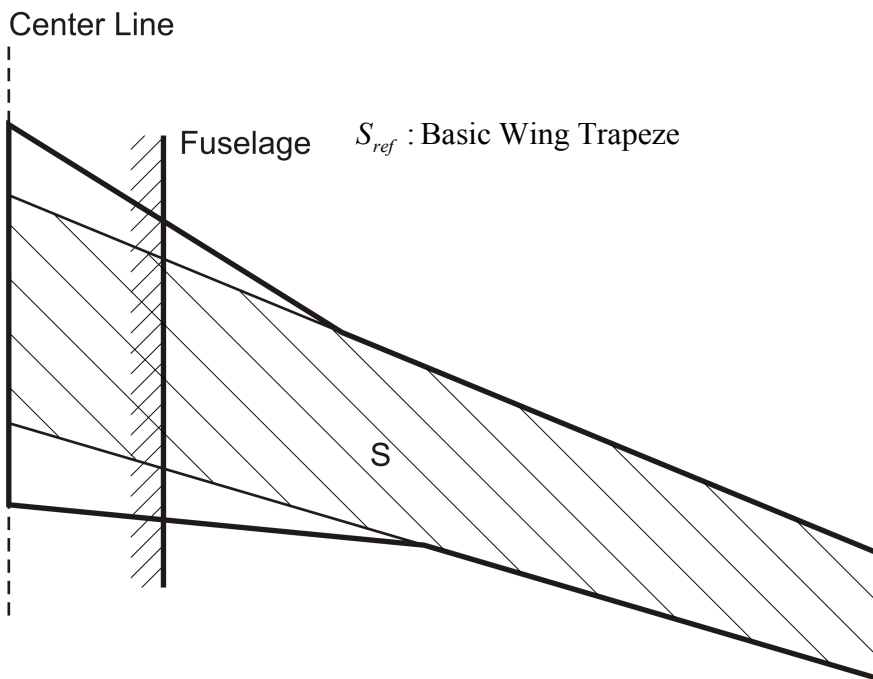


**Fig. 7.4**

a)  
Definition of the reference wing area according to Boeing.

Note: The Boeing B-747 has a different definition of the reference wing area:  $S_{ref} = S$ .



b)  
Definition of the reference wing area according to Fockler and McDonnell Douglas.

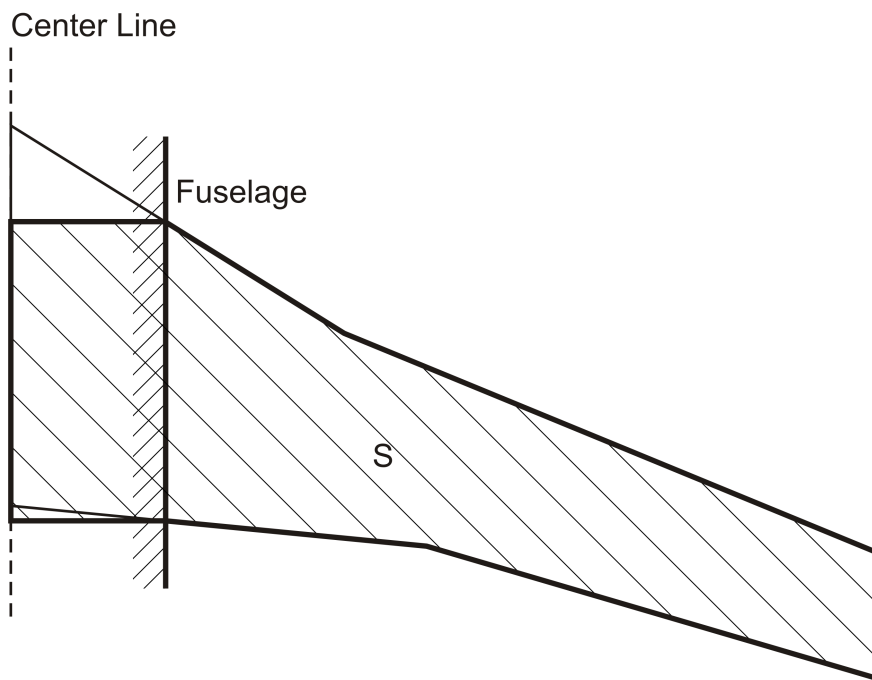


**Fig. 7.5**  
Definition of the reference wing area according to Airbus

### Wing parameters in aircraft design

The following have **already been determined** (to a large extent) (see Section 5):

- Wing area  $S_w$
- Wing aspect ratio  $A_w$ .

When searching for a suitable aircraft configuration (see Section 4) consideration was already given to transmitting the forces from the wing to the fuselage by means of the following configuration:

- cantilever wing
- braced wing

and to the position of the wing in relation to the fuselage

- low wing position
- mid wing position
- high wing position

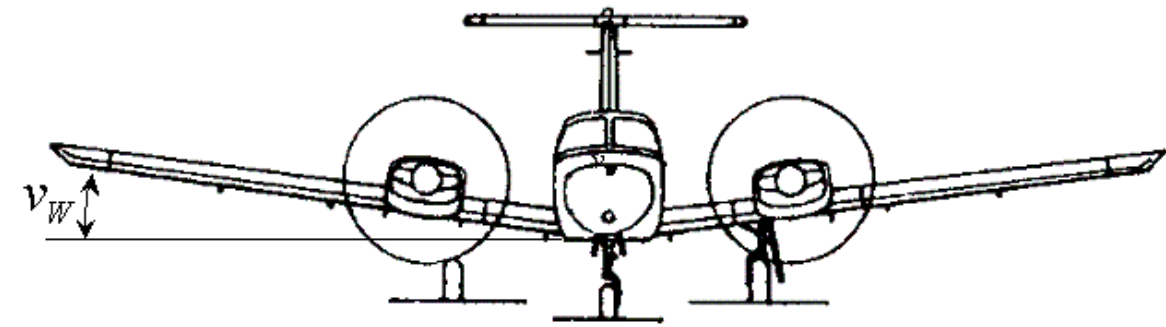


**Fig. 7.6** (Positive) dihedral angle of the wing  $v_W$

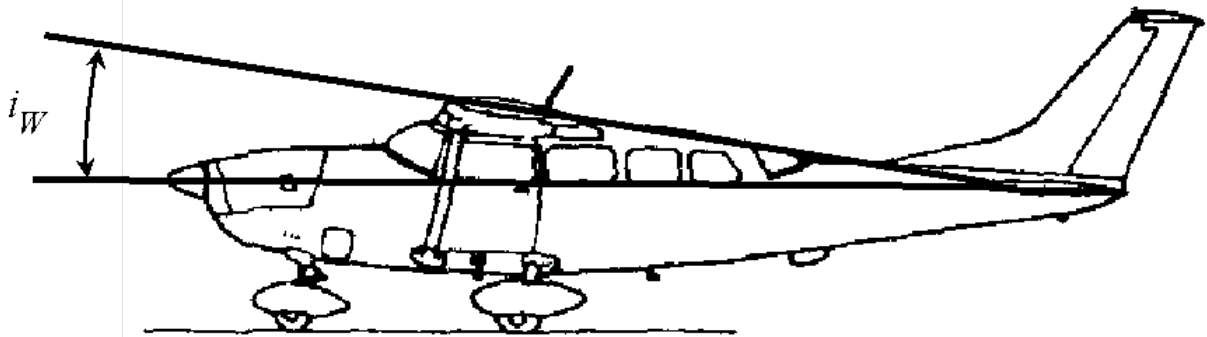


**Fig. 7.7** (Positive) incidence angle  $i_W$ : angle between the chord line of the wing root and a reference line of the fuselage (e.g. cabin floor)

The following still have **to be determined** (here in Section 7):

Taper ratio,  $\lambda_W$

Sweep angle,  $\phi_{25,W}$

Thickness ratio,  $(t/c)_W$

Airfoils

Dihedral angle,  $v_W$  (**Fig. 7.6**)

Incidence angle,  $i_W$  (**Fig. 7.7**)

Wing twist,  $\varepsilon_t$  (**Fig. 7.8**)

Subsections 7.2 and 7.3 below contain equations and estimates for these parameters. It is important to compare and check the calculation results with the values from the aircraft statistics. Tables with wing parameters are, for example, included in **Roskam II** (Section 6) and **Torenbeek 1988** (Section 7). Further comprehensive information can be found in “Jane's All The World's Aircraft” (**Lambert 1993**).

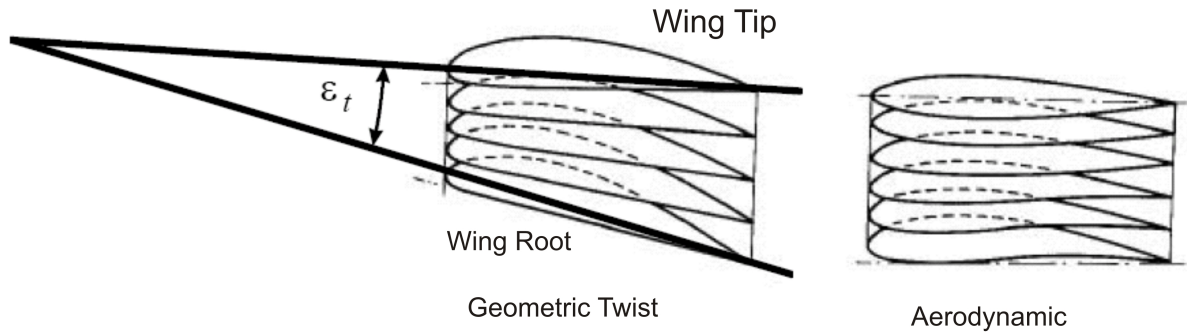


**Fig. 7.8** Wing twist  $\epsilon_t$ . The twist shown in the diagram is negative. There are two types of wing twist:

- 1.) Geometric twist:  
change in the angle between the chord lines.
- 2.) Aerodynamic twist:  
change in the zero-lift line along the span of an airfoil.  
The diagram shows the typical case of reduced lift at the wing tip, i.e. "wash out".  
The opposite effect is called "wash in".

The following must be **taken into account** when choosing parameters:

- Take-off/landing: maximum lift coefficient, required high lift systems, lift-to-drag ratio, attitude, lift curve slope  $dC_L / d\alpha$
- Cruise: lift-to-drag ratio  $L/D$ , drag divergence Mach number  $M_{DD}$ , buffet onset boundary
- Fuel tank volume
- Flight characteristics, stalling behavior, flight in turbulence
- Landing gear actuation and stowage
- Wing mass
- Production costs

These characteristics, which depend on the choice of the above-mentioned wing parameters, are discussed in Subsection 7.3.

## Definitions

*Aspect ratio*

$$A = \frac{b^2}{S} \quad , \quad (7.1)$$

with Span  $b$ .

*Mean aerodynamic chord*

$$c_{MAC} = \frac{2}{S} \int_0^{b/2} c^2 dy \quad , \quad (7.2)$$

*Area*

$$S = 2 \int_0^{b/2} c \, dy \quad , \quad (7.3)$$

*Spanwise location of mean aerodynamic chord*

$$y_{MAC} = \frac{2}{S} \int_0^{b/2} c \cdot y \, dy \quad . \quad (7.4)$$

with  $y$  spanwise location.

*Relative span position*

$$\eta = \frac{y}{b/2} \quad , \quad (7.5)$$

*Taper ratio*

$$\lambda = \frac{c_t}{c_r} \quad , \quad (7.6)$$

The following additionally applies to double tapered wings:

on the inner wing (index:  $i$ )  $\lambda_i = \frac{c_k}{c_r} \quad , \quad (7.7)$

on the outer wing (index:  $o$ )  $\lambda_o = \frac{c_t}{c_k} \quad . \quad (7.8)$

**Equations for the geometry of the simple tapered wing**

$$A = \frac{b^2}{S} = \frac{2b}{c_r(1+\lambda)} \quad , \quad (7.9)$$

$$c_{MAC} = \frac{2}{3} c_r \frac{1+\lambda+\lambda^2}{1+\lambda} \quad , \quad (7.10)$$

$$S = \frac{b}{2} c_r (1+\lambda) \quad , \quad (7.11)$$

$$\frac{y_{MAC}}{b/2} = \frac{1 - \frac{c_{MAC}}{c_r}}{1 - \lambda} = \frac{1}{3} \left( \frac{1+2\lambda}{1+\lambda} \right) \quad , \quad (7.12)$$



Conversion of the sweep of an  $m\%$  line to the sweep of an  $n\%$  line (m and n are the % values):

$$\tan \varphi_n = \tan \varphi_m - \frac{4}{A} \left[ \frac{n-m}{100} \cdot \frac{1-\lambda}{1+\lambda} \right] \quad (7.13)$$

### Equations for the geometry of the double tapered wing

$$A = \frac{b^2}{S} = \frac{2b}{c_r [(1-\lambda) \cdot \eta_k + \lambda_i + \lambda]} \quad (7.14)$$

with

$$\eta_k = \frac{y_k}{b/2} \quad .$$

$$c_{MAC} = \frac{c_{MAC,i} \cdot S_i + c_{MAC,o} \cdot S_o}{S} \quad (7.15)$$

$$S = S_i + S_o = \frac{b^2}{A} = \frac{b}{2} c_r [(1-\lambda) \cdot \eta_k + \lambda_i + \lambda] \quad (7.16)$$

$$y_{MAC} = \frac{y_{MCA,i} \cdot S_i + (y_k + y_{MAC,o}) \cdot S_o}{S_i + S_o} \quad (7.17)$$

Please note: The index  $( )_w$  for wing was omitted in equations 7.1 to 7.16 because the equations are thus also applicable to a horizontal tailplane. When calculating the geometry of a vertical tailplane, it is important to take into account that the tailplane only consists of half the area. Thus, for example, equation (7.3) can be used to produce the definition for the area of the vertical tailplane  $S_V$  :

$$S_V = \int_0^{b/2} c \, dy \quad (7.17)$$

## 7.2 Basic Principle and Design Equations

### Pressure coefficient

The flow configurations around an airfoil are shown with the aid of the pressure coefficient (see Fig. 7.12). The **pressure coefficient** is defined as

$$c_p = \frac{p - p_\infty}{q_\infty} \quad (7.18)$$

The index “ $\infty$ ” refers to a parameter of the free flow (undisturbed by the airfoil section). By definition:  $q_\infty = \frac{1}{2} \rho V_\infty^2$  and for incompressible flow (Bernoulli)  $p_\infty + \frac{1}{2} \rho V_\infty^2 = p + \frac{1}{2} \rho V^2$  hence  $p - p_\infty = \frac{1}{2} (\rho V_\infty^2 - \rho V^2)$ . With the local *super velocity*  $v = V - V_\infty$

$$c_p = \frac{\frac{1}{2} \rho \cdot (V_\infty^2 - V^2)}{\frac{1}{2} \rho V_\infty^2} = 1 - \left( \frac{V}{V_\infty} \right)^2 \approx - \frac{2 \cdot v}{V_\infty} \quad (7.19)$$

The approximation ( $\approx$ ) applies for  $v$  much smaller than  $V_\infty$ . The local velocity at the airfoil is

$$V = V_\infty \cdot \sqrt{1 - c_p} \quad (7.20)$$

For compressible flow, the equation is as follows, with the ratio of specific heats  $\gamma$ :

$$c_p = \frac{2}{\gamma \cdot M} \left[ \left( \frac{2 + [\gamma - 1] \cdot M_\infty^2}{2 + [\gamma - 1] \cdot M^2} \right)^{\frac{\gamma}{\gamma - 1}} - 1 \right] \approx - \frac{2 \cdot v}{V_\infty} \quad (7.21)$$

The derivation and background to equation (7.21) can be found e.g. in **Anderson 1991**.

### Mach number correction

From a flow speed of approximately  $M = 0.3$ , it is necessary to correct coefficients such as  $c_p$ ,  $c_L$ ,  $c_D$ . This can be done with the aid of the Prandtl-Glauert compressibility correction, as is shown here using the example of the pressure coefficient:

$$c_p = \frac{c_{p, M=0}}{\sqrt{1 - M_\infty^2}} \quad (7.22)$$

The **Mach number correction factor according to Prandtl-Glauert** is therefore  $\frac{1}{\sqrt{1 - M_\infty^2}}$ ,

but it only applies to

- 2-dimensional flow (i.e. for airfoils),
- thin airfoil sections,
- small angles of attack,
- pure subsonic flow, i.e. for  $M < M_{crit}$ . (See below for a definition of  $M_{crit}$ ).

Despite these restrictions, the Mach number correction according to Prandtl-Glauert is often used as the first approximation.

### Lift curve slope

The lift curve slope gives the increase in the lift coefficient with the angle of attack

$$C_{L,\alpha} = \frac{dC_L}{d\alpha} \quad (7.23)$$

The **lift curve slope of a wing** is calculated here according to **DATCOM 1978** (Section 4.1.3.2). Corrections will be necessary for the combination of wing-fuselage and wing-fuselage-empennage.  $C_{L,\alpha}$  is calculated from the equation in 1/radian [1/rad].

$$C_{L,\alpha} = \frac{2 \cdot \pi \cdot A}{2 + \sqrt{\frac{A^2 \cdot \beta^2}{\kappa^2} \cdot \left(1 + \frac{\tan^2 \varphi_{50}}{\beta^2}\right) + 4}} \quad (7.24)$$

$\beta$  is the reciprocal of the Mach number correction factor

$$\beta = \sqrt{1 - M^2} \quad (7.25)$$

and

$$\kappa = \frac{C_{L,\alpha}}{2\pi / \beta} \quad (7.26)$$

Some authors use  $\kappa = 1$  for simplicity's sake and obtain the following from equation (7.24)

$$C_{L,\alpha} = \frac{2 \cdot \pi \cdot A}{2 + \sqrt{A^2 \cdot (1 + \tan^2 \varphi_{50} - M^2) + 4}} \quad (7.27)$$

In equation (7.26) for equation (7.24),  $C_{L,\alpha}$  is the **lift curve slope of the airfoil section**.  $C_{L,\alpha}$  can be estimated from

$$c_{L,\beta} = \frac{1.05}{\beta} \cdot \left[ \frac{c_{L,\beta}}{(c_{L,\beta})_{theory}} \right] \cdot (c_{L,\beta})_{theory} \tag{7.28}$$

with data from Fig. 7.9 and with the theoretical lift curve slope of the airfoil

$$(c_{L,\beta})_{theory} = 2 \cdot \pi + 4.7 \cdot (t/c) \cdot [1 + 0.00375 \cdot \Phi_{TE}] \tag{7.29}$$

In equation (7.29),  $\Phi_{TE}$  is the trailing edge angle according to Fig. 7.2 in degrees. Equation (7.29) gives the result  $(c_{L,\beta})_{theory}$  in 1/radian [1/rad].

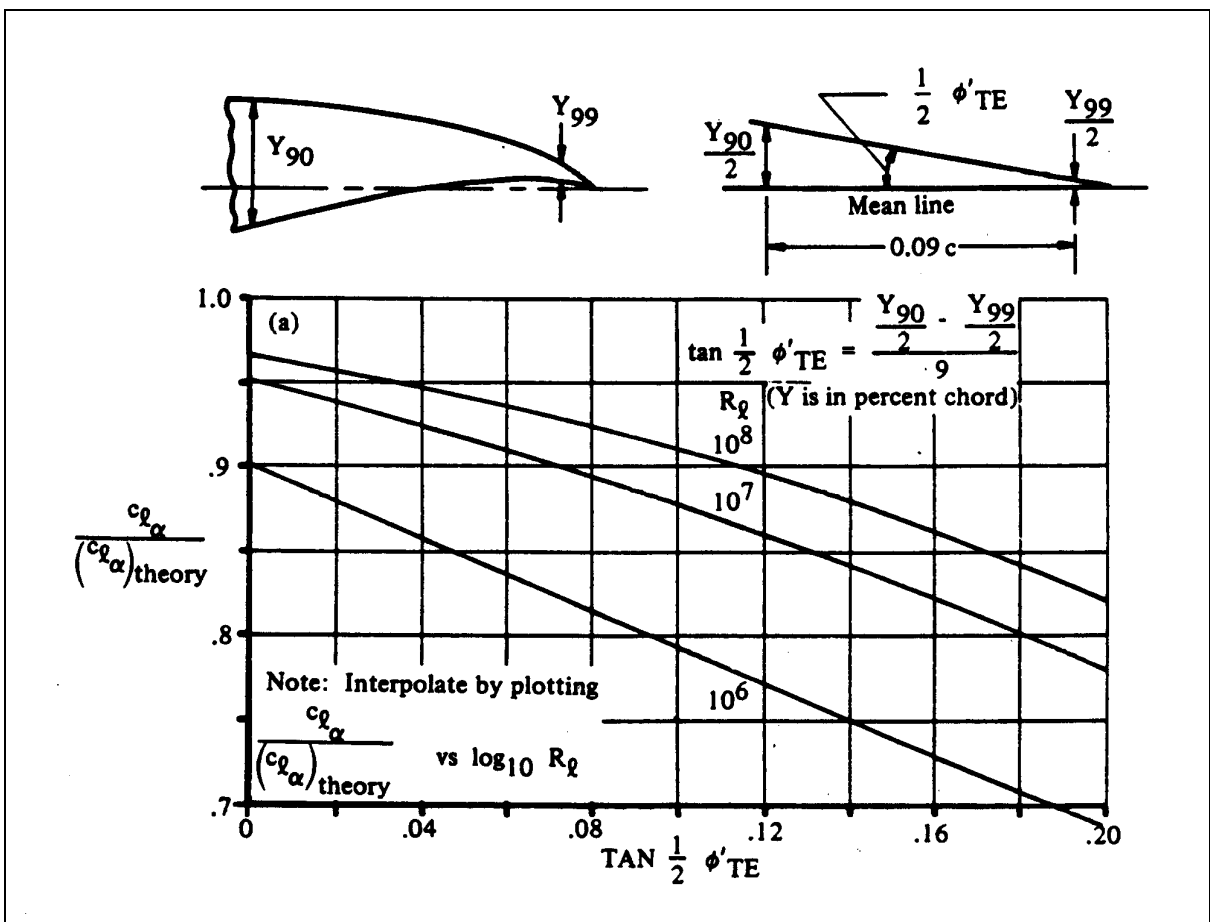
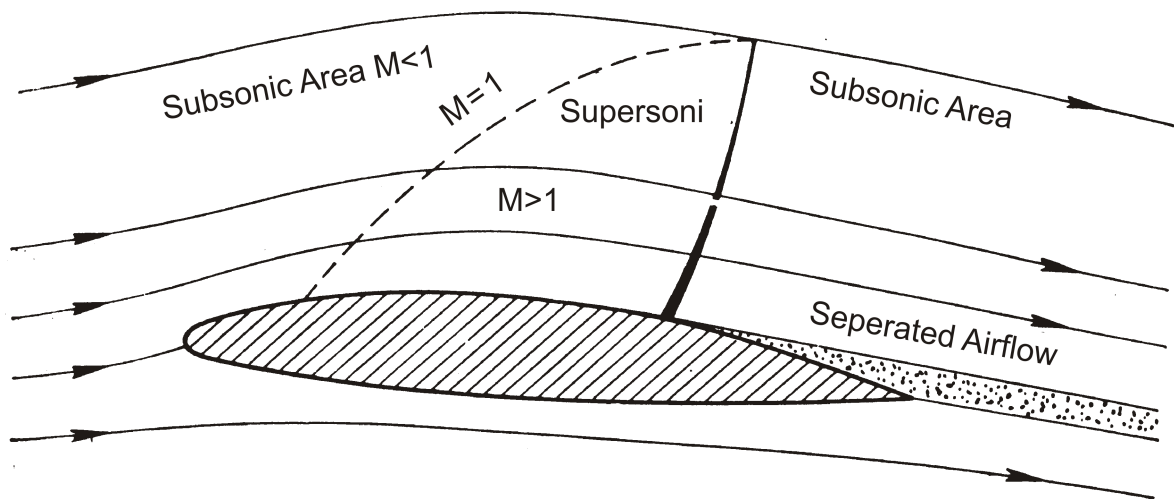


Fig. 7.9 Calculating the lift curve slope of an airfoil section according to DATCOM 1978

### Critical Mach number and shock wave

If the flight Mach number  $M$  is increased to close to  $M = 1$ , the **flow speed** in the vicinity of the airfoil will at some point **exceed the speed of sound** (i.e. exceed  $M = 1$ ). The flight Mach number achieved at this point is called the *critical Mach number*  $M_{crit}$ . The critical Mach number is smaller than 1 because, due to the super velocities  $v$ , the local flow speeds may be

higher than the airspeed. According to equation (7.21), one would expect the super velocities to occur where there are negative pressure coefficients – i.e. on the suction or upper surface of the airfoil. After the critical Mach number has been exceeded a localized area with  $M > 1$  appears first on the upper surface of the airfoil and only later on the lower surface as well (see **Fig. 7.10**). As this local flow  $M > 1$  finally recombines with the free stream behind the airfoil, it has to be reduced to  $M < 1$  again at some point. This reduction involves an increase in pressure. A *shock wave* occurs. In the shock wave, the local Mach number drops from an initial value of  $M > 1$  to a value of  $M < 1$ . The shock wave leads to an **increase in the drag and to the separation of the boundary layer**. As the Mach number increases, the shock waves above and below the airfoil section move more and more to the rear. If the flow speeds increase even further, the shock waves are finally located at the end of the airfoil section and form the so-called “wake”.



**Fig. 7.10** Airfoil section subjected to subsonic flow speed  $M_{crit} < M < 1$ . After the flow has passed through the supersonic area, the flow is then decelerated in the shock wave from a local speed  $M > 1$  to a speed  $M < 1$

### Drag divergence Mach number

The parameters of a wing must be chosen so as to ensure that the drag increase of the aircraft is not too high at the required cruise Mach number  $M_{CR}$ . As the Mach number increases, the critical Mach number  $M_{crit}$  will first be reached. This is the flight Mach number where the speed of sound occurs locally at the wing for the first time (see above). The drag divergence Mach number  $M_{DD}$  is – according to a definition applied by Airbus and Boeing – the Mach number where the wave drag (that is the additional drag due to Mach effects) amounts to 0.0020.  $M_{DD}$  is larger than  $M_{crit}$ . How much bigger depends on the type of airfoil section. Typically,  $M_{DD}$  is 0.08 Mach higher than the critical Mach number  $M_{crit}$  (**Raymer 1989**).

The increase in drag, caused by the wave drag, is shown in **Fig. 7.11**. At  $M = 1.0$ , the drag is only approximately half as big as at  $M = 1.2$  or at  $M = 1.05$ . The wave drag at  $M = 1.05$  is approximately as big as the wave drag at  $M = 1.2$ .

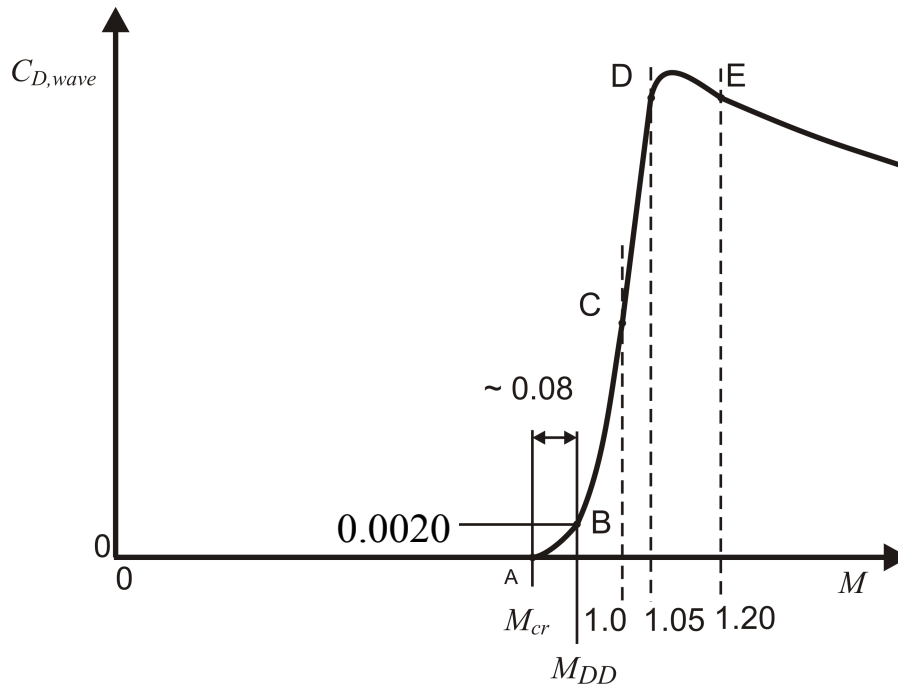


**Fig. 7.11**  
A typical progression of the wave drag  $C_{D,wave}$  as a function of the flight Mach number  $M$

The drag divergence Mach number  $M_{DD}$  rises with

- decreasing lift coefficient  $C_L$ ,
- decreasing relative thickness ( $t/c$ ),
- increasing leading edge radius,
- increasing sweep  $\phi$ .

### Transonic airfoils

Special transonic airfoils (called “supercritical airfoil” by NASA) increase the cruise Mach number or allow the use of a larger relative thickness. Through a larger relative thickness, the wing weight can be reduced and therefore, at the end of the day, the operating costs are also cut.

During the Second World War, airfoils were already being developed with a view to increasing the critical Mach number. In particular, **NACA 6-series sections (Abbott 1959)** showed improvements in the drag increase at high Mach numbers without having too detrimental an effect on the slow flight characteristics. These airfoils were used in the first generation of subsonic jet aircraft, such as for the Caravelle.

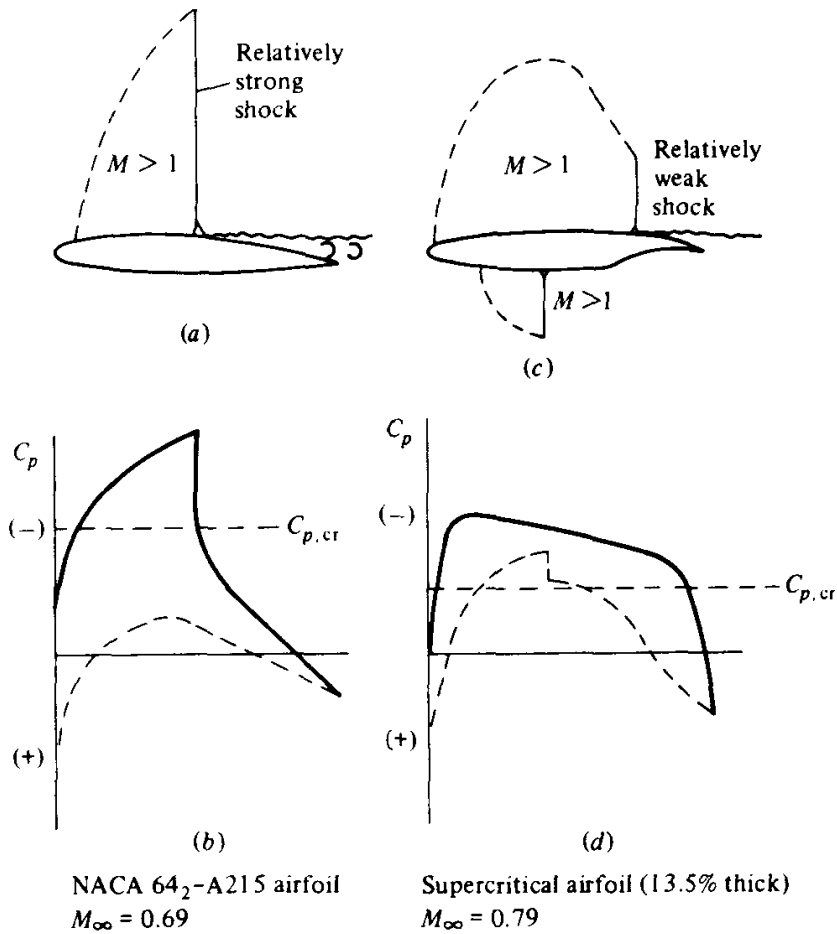
The first airfoils for the supercritical area were the **sections with peaky pressure distribution** from PEARCY in England. It was already known that by means of thinner sections,  $M_{crit}$  could be increased. The idea was to increase the distance between  $M_{crit}$  and  $M_{DD}$ . This was achieved by a virtually isentropic pressure increase prior to a weak shock wave. The drag increase could thereby be delayed by  $M = 0.02$  to  $0.03$  compared to the airfoils of the NACA 6 series. This type of airfoil was used, for example, in the BAC 1-11, VC-10 and DC-9.

At the start of the sixties, WHITCOMB at NASA was working on **supercritical sections**. His work still forms the basis for the airfoils used in civil transports and business jets.

**Fig. 7.12** compares a conventional airfoil with a supercritical airfoil. With the conventional airfoil, the flow on the upper surface of the airfoil section is accelerated even more after the speed of sound has been exceeded locally, so that a strong shock wave is created approximately in the middle of the airfoil. Due to the strong increase in pressure in the shock wave, separation of the flow occurs with a large increase in drag and stochastic force fluctuations on the wing. This phenomenon is called buffeting. On the other hand, in the case of the supercritical airfoil, a uniform supercritical distribution of pressure occurs at a lower level, which is concluded by a weaker shock wave in the rear section of the airfoil.

Supercritical airfoils differ from conventional airfoils in the following ways:

1. The **upper surface of the airfoil is only slightly curved in the middle section**. Therefore the low pressure, and thus also the flow speed, is reduced, so that the shock wave is shifted to the trailing edge and the intensity of the impact shock can be reduced.
2. The **lower surface of the airfoil has a concave curvature in the rear section** with a so-called S shock. This produces a greater increase in pressure, which increases the lift with the same angle of attack and therefore allows a reduced angle of attack for the required lift, thus taking the strain off the upper surface of the airfoil (rear loading). The rear loading, however, leads to a not insignificant pitching moment, which must be compensated for by correspondingly larger empennages.
3. The **leading edge radius of the section is increased** to avoid excessive super velocities.
4. The **airfoil leading edge** may also be curved downward somewhat. This means that acceptable lift coefficients can be achieved in slow flight – despite the disadvantage of having only a slight curvature in the middle section of the airfoil.

**Fig. 7.12**

Standard airfoil of the NACA 6 series compared to a supercritical airfoil at cruise Mach number (Andersen 1991)

### High-altitude flight and buffet onset boundary

At high altitudes the speed of sound is low, and therefore the Mach number is high for a given airspeed. Due to the low air density, a high lift coefficient and a high angle of attack are necessary. A flight in gusty air or with maneuvers such as a turn requires still higher lift coefficients and angle of attack. In doing so, the aircraft may **stall** (the aircraft is too *slow*). On the other hand, the Mach number may be too high for the required lift coefficient, so that **buffeting** occurs (the aircraft is too *fast*). As shown in **Fig. 7.13**, the usable speed range becomes more and more limited as the altitude increases. When designing the wing, this phenomenon must be taken into account. It is important to ensure that a usable airspeed range is retained at cruise altitude.



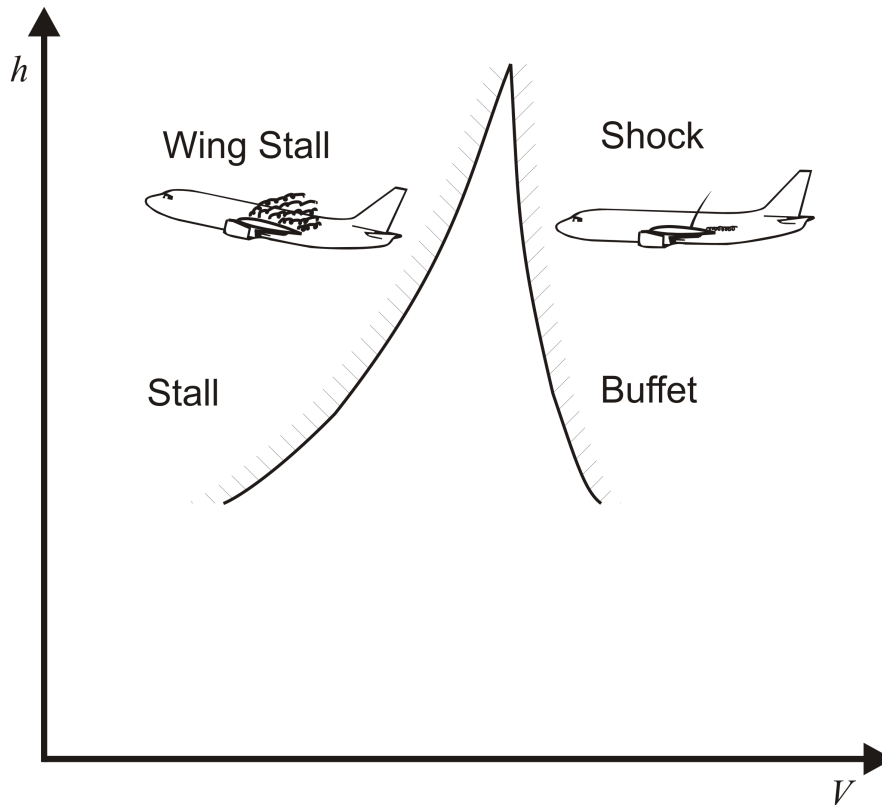


**Fig. 7.13:** Stall boundary and buffet boundary. The usable speed range becomes smaller as the altitude increases

The certification regulations contain the following requirements:

CS 25.251	Vibration and buffeting
(b)	Each part of the aeroplane must be shown in flight to be <b>free from excessive vibration</b> , under an appropriate speed and power conditions <b>up to</b> at least the minimum value of <b>VD</b> allowed in CS 25.335.
(d)	There may be <b>no perceptible buffeting</b> condition in the cruise configuration in straight flight at any speed <b>up to VMO/MMO</b> ...

ACJ 25.1585(c)	Cruise Maneuvering Capability
	... it is possible to achieve a positive normal <b>acceleration increment of 0.3 g</b> without exceeding the <b>buffet onset</b> boundary ...

In cruise flight up to  $V_{MO}$  (maximum operating limit speed) or  $M_{MO}$  (maximum operating limit Mach number) with a load factor of 1.3g, no buffeting may occur. Up to  $V_D$  (design diving speed) or  $M_D$  (design diving Mach number) ( $M_D$  is approximately 0.05 to 0.09 above  $M_{MO}$ ) acceptable flying characteristics must be retained. Buffeting is, however, allowed. Unfortunately, there is no simple way to calculate the buffet onset boundary.

### Calculation of wing parameters from the design Mach number

**Airbus** and **Boeing** use the following design Mach number (= cruise Mach number)

$$M_{design} = M_{CR} :$$

$$M_{DD} = M_{CR} \quad (7.30)$$

and thereby obtains (by definition, see above) a wave drag of 0.002.

There are certainly other possibilities to place  $M_{DD}$  with respect to  $M_{CR}$ . **Obert 1997** (reporting from experience at **Fokker**) recommends setting the cruise Mach number so as to achieve a wave drag of 0.0015. If we bear in mind that  $M_{DD} = M_{crit} + 0.08$  (see Fig. 7.11), roughly the following applies:

$$M_{DD} \approx M_{CR} + 0.02.$$

As we can see, to some extent it is up to the design engineer to set the drag divergence Mach number  $M_{DD}$  in relation to the required cruise Mach number  $M_{CR}$ .

The **effective Mach number** and **effective speed** for a swept wing are according to the geometric considerations and the **cosine rule** from **Fig. 7.14**:

$$V_{eff} = V \cdot \cos \phi_{25} \quad \text{and} \quad M_{eff} = M \cdot \cos \phi_{25}$$

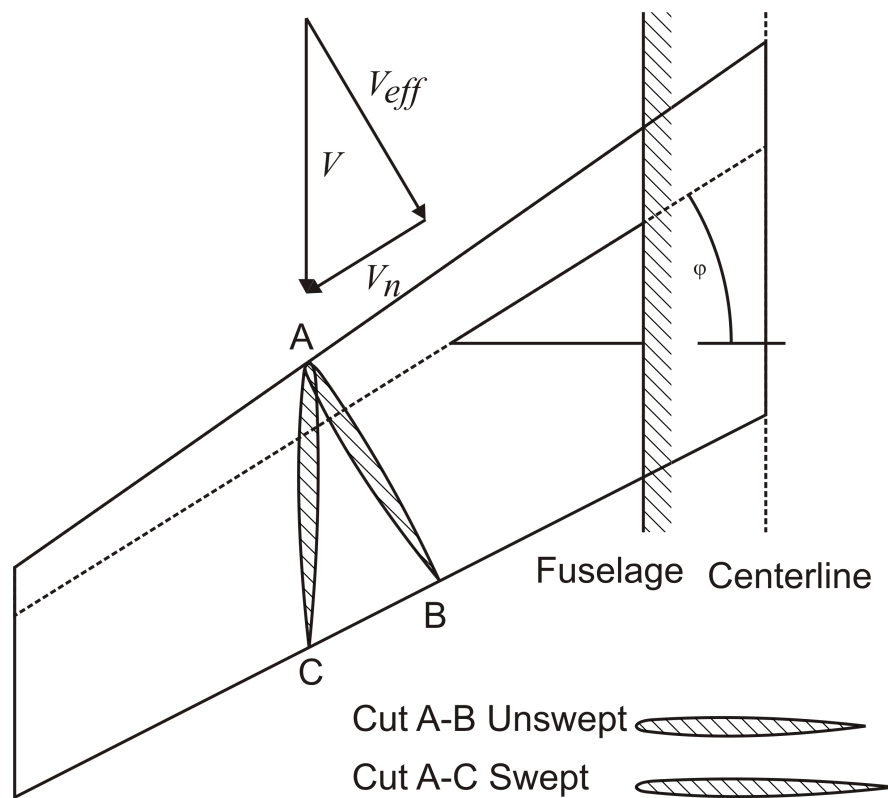


**Fig. 7.14:** Decomposition of the vector  $V$  of the flow speed into an effective component perpendicular to the wing (index: eff) and a component along the wing quarter chord line (index: n)

Furthermore it is

$$c_{eff} = c \cdot \cos \phi_{25} \quad ,$$

$$t_{eff} = t \quad ,$$

$$(t/c)_{eff} = (t/c) / \cos \phi_{25} \quad .$$

However, experience has shown that sweep does not enable the effective Mach number to be reduced as much as the geometric considerations would lead one to assume. Therefore the following general equation is used:

$$M_{eff} = M \cdot (\cos \phi_{25})^x \quad (7.31)$$

The cosine rule corresponds to  $x = 1.0$

STAUFENBIEL suggests:  $x = 0.75$ .

**Torenbeek 1988** and many other authors suggest:  $x = 0.5$ .

If we stick with **Torenbeek 1988** and  $x = 0.5$ , then the following also applies:

$$M_{DD,eff} = M_{DD} \cdot \sqrt{\cos \phi_{25}} \quad (7.32)$$

Bearing in mind that  $(t/c) = (t/c)_{eff} \cdot \cos \phi_{25}$  applies, according to **Torenbeek 1988** the maximum permissible relative thickness of an airfoil parallel to the aircraft's plane of symmetry is as follows:

$$(t/c) = 0.3 \cdot \cos \phi_{25} \cdot \left( \left[ 1 - \left( \frac{5 + M_{DD,eff}^2}{5 + (k_M - 0.25 \cdot C_L)^2} \right)^{3.5} \right] \cdot \frac{\sqrt{1 - M_{DD,eff}^2}}{M_{DD,eff}^2} \right)^{\frac{2}{3}} \quad (7.33)$$

$k_M = 1.00$	conventional airfoils; maximum $t/c$ at about $0.30c$ ,
$k_M = 1.05$	high-speed (peaky) airfoils, 1960-1970 technology,
$k_M = 1.12$ to $1.15$	supercritical airfoils.
$C_L$ :	the design lift coefficient (for cruise) chosen in Section 5

The calculated  $t/c$  applies for an average spanwise position on the wing. **Jenkinson 1999** calculates an average relative thickness from the relative thickness at the tip ( $t$ ) and root ( $r$ ) of the wing:

$$t/c = \frac{3(t/c)_t + (t/c)_r}{4} \quad .$$

The accuracy of the calculation (estimation) of relative thickness turns out to be limited with simple equations like (7.33). Further information on calculating the maximum permissible relative thickness of a wing can be found in **Scholz 2005**.

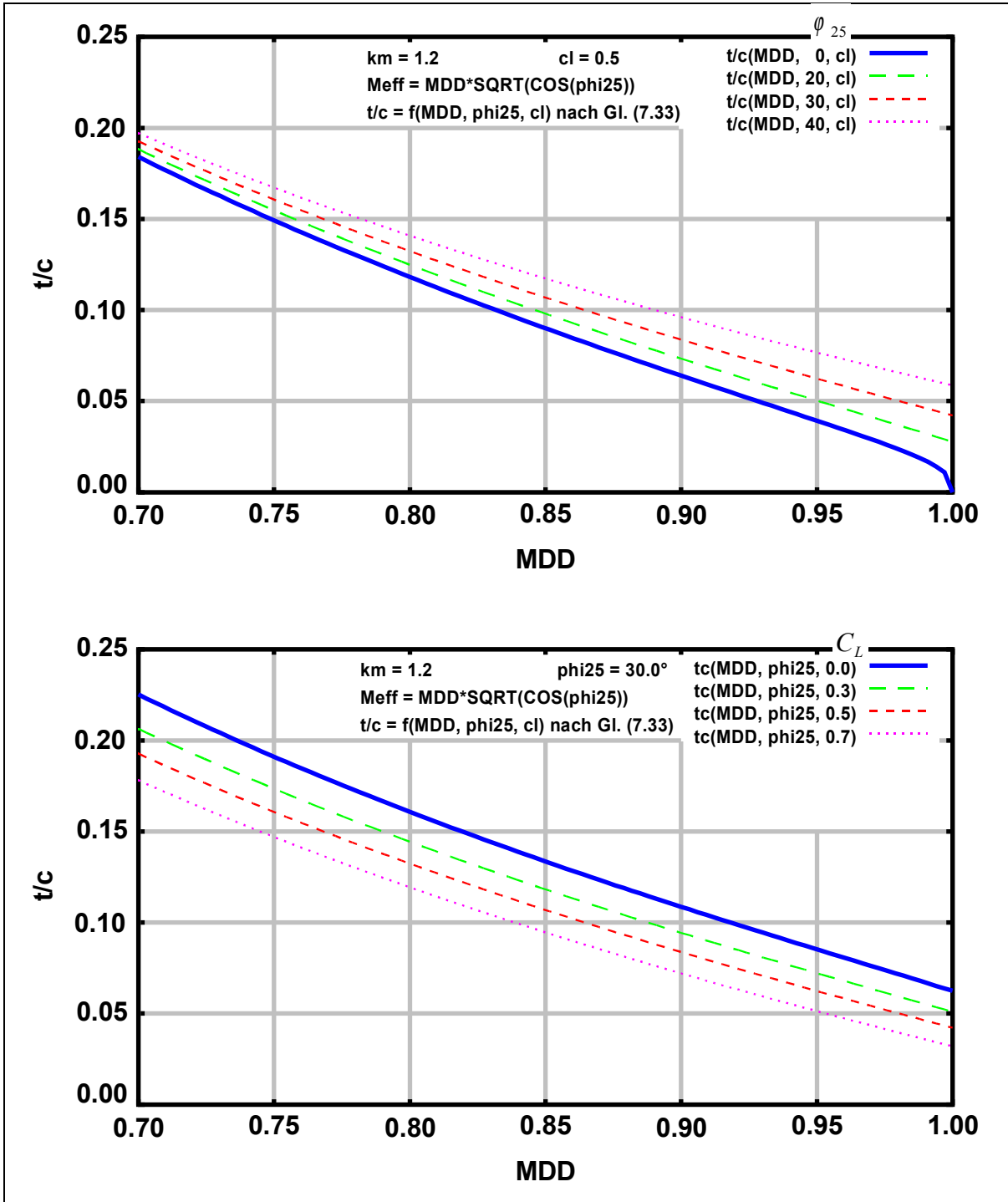


**Fig. 7.15 (top) and Fig. 7.16 (bottom)**

Influence of drag divergence Mach number  $M_{DD}$  on the relative thickness  $t/c$  using sweep angle  $\phi_{25}$  (top) and of the design lift coefficient  $C_L$  (bottom) as further parameter. Calculated with equation (7.32) and (7.33)

**Fig. 7.15** shows the influence of  $M_{DD}$ ,  $\phi_{25}$  and  $C_L$  on  $t/c$ . Fig. 7.15 was calculated with equations (7.32) and (7.33).

## Winglets and End Plates

The effective aspect ratio can be increased by means of winglets without increasing the span. This can make sense if the span is limited due to the structural specifications of the airfield, hangar or gate. The effective span for a wing with winglets or end plates can be estimated according to **Dubs 1987** with

$$A_{eff} = A / (1 + \delta_E) \quad (7.34)$$

with  $(1 + \delta_E)$  from **Fig. 7.18** according to the geometry from **Fig. 7.17**.

Practical note: In Section 5 an aspect ratio was used to determine the glide ratio  $L/D$  in cruise configuration. This aspect ratio may now be considered as the effective aspect ratio. ( 7.34 ) may now be used to calculate the geometric aspect ratio from

$$A = A_{eff} (1 + \delta_E) .$$

It follows the span from

$$b = \sqrt{A S_W} .$$

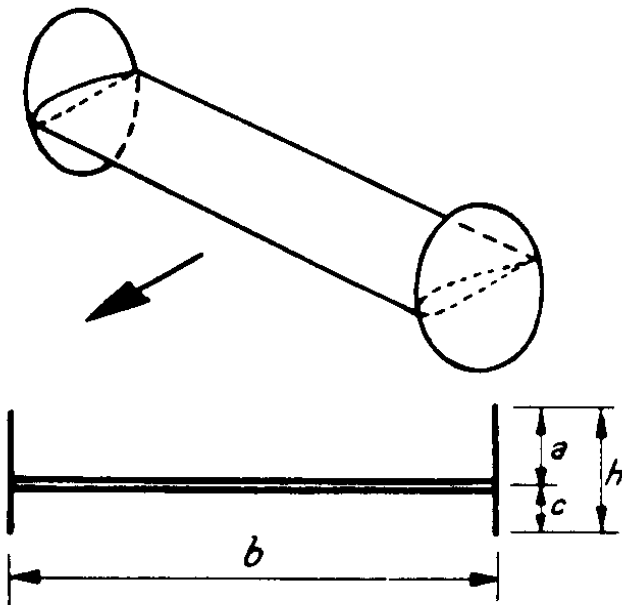


**Fig. 7.17**

Geometry of a wing with winglets or end plates (**Dubs 1987**)

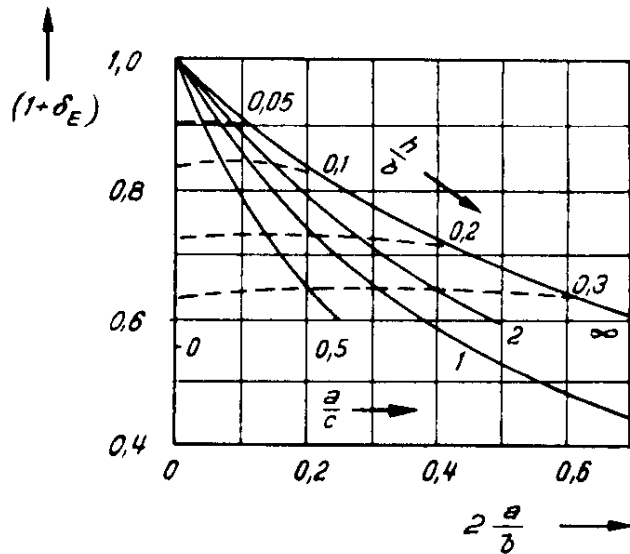


Fig. 7.18

Factor for calculating the effective aspect ratio of a wing with winglets or end plates (Dubs 1987)

### Volume of the fuel tank

Torenbeek 1988 specifies a semi-empirical equation for estimating the volume of the fuel tank. This equation is reported to have a degree of precision of  $\pm 10\%$ .

$$V_{\text{tank}} = 0.54 \cdot S_W^{1.5} \cdot (t/c)_r \cdot \frac{1}{\sqrt{A}} \cdot \frac{1 + \lambda \cdot \sqrt{\tau} + \lambda^2 \cdot \tau}{(1 + \lambda)^2} \quad (7.35)$$

with

$$\tau = \frac{(t/c)_t}{(t/c)_r}$$

When deriving the equation, it was assumed that a simple tapered wing was involved with a linear thickness distribution. Statistical data was used to calculate the correction factor of 0.54. The sweep has virtually no impact on the tank volume. Equation (7.35) can also be used to calculate the tank volume of a tank that only covers part of the span of the wing. The parameters of the wing root  $r$  and the wing tip  $t$  then have to be set to the values on the inner and outer end of the tank.

## 7.3 Flight and Operational Characteristics

### Cantilever or braced wing

Braced wings can be constructed so that they are approximately 30% lighter than cantilever wings. However, the struts cause considerable form and interference drag. They are therefore

only used for comparatively slow aircraft (less than approximately 200 kt). An aircraft configuration with joint wings (see Section 4) tries to achieve both advantages simultaneously.

### Position of the wing in relation to the fuselage

The optimum position of the wing in relation to the fuselage depends on the type of aircraft use. In the case of a **cargo aircraft**, the emphasis is on ease of loading and unloading. If the aircraft is to be loaded directly from a lorry or by using an on-board ramp, a high-wing aircraft is required. In the case of a **passenger aircraft**, the high-wing offers passengers good visibility. However, landing gear mounted on the wing will be heavy in the case of the high wing aircraft due to its length. Landing gear mounted on the fuselage will require additional drag-inducing fuselage cladding. In most cases, a mid-wing configuration is not possible on passenger and cargo aircraft because it would prevent a continuous free cross section for the cabin or the hold. **Seaplanes** achieve the necessary distance between the wing and the water surface by means of a high wing configuration. For **small aircraft**, no wing position has established itself as the best compromise up to now. In general the following applies:

- A mid-wing configuration creates the least interference drag. (Interference drag is produced by the mutual influence of the airflow over the fuselage and wing).
- The high positioning of the wing has a stabilizing effect around the rolling axis (**Fig. 7.19**), but has a destabilizing influence on Dutch roll. Aft swept wings also have a positive stabilizing effect around the longitudinal axis and a positive dihedral angle. The connections are assessed in the subsection “Dihedral”.

**Table 7.1** Summary evaluation of wing position in relation to the fuselage

	High wing	Mid wing	Low wing
<b>Interference drag</b>	average	low	high
<b>Stability around the longitudinal axis</b>	stable	neutral	unstable (requires dihedral for stability)
<b>Visibility from cabin and cockpit <sup>a</sup></b>	good	average	poor
<b>Landing gear: on the wing</b>	long and heavy	-	short and light
<b>on the fuselage</b>	high drag	-	-
<b>Loading</b>	easy	average	requires steps and loading aids

<sup>a</sup> Visibility depends on where the wing cuts through the fuselage.

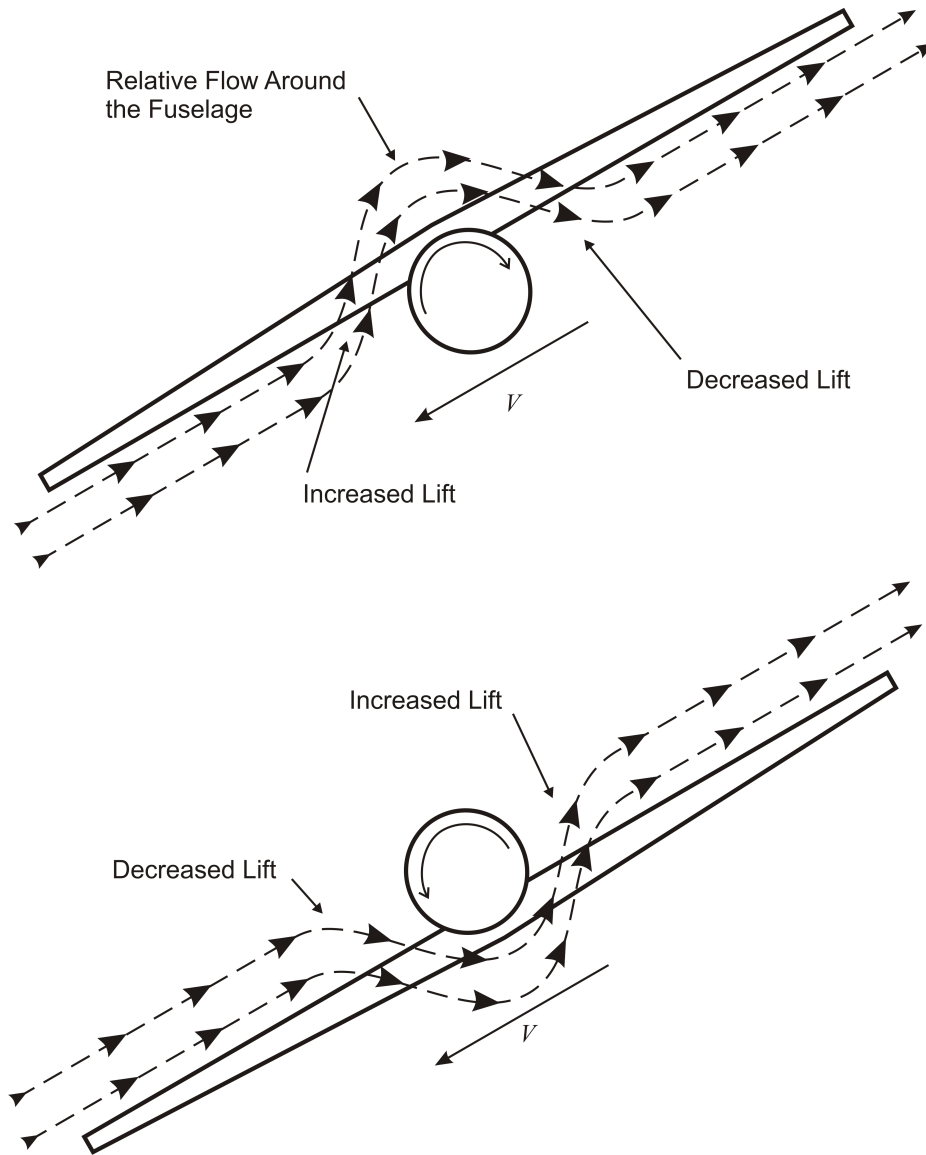


**Fig. 7.19** Effect of wing position on roll stability

### Wing area and wing loading

The wing area was determined from the requirements to be met by the aircraft in the **preliminary sizing**. Then the smallest possible thrust-to-weight ratio and the smallest possible wing were chosen, and consequently the highest possible wing loading. In doing so, it was assumed that **the larger the area of a wing, the heavier and more expensive** it becomes.

If a specific **approach speed** or a specific **landing distance** is not to be exceeded, the wing area should not be too small.



In the case of a **flight in turbulent air** the aircraft is especially influenced by vertical gusts. These vertical gusts momentarily change the wing's angle of attack. For example, the angle of attack is increased by a vertical gust from below (in addition to the flow acting on the wing due to the airspeed). The aircraft's response to the vertical gust is expressed by the change in the load factor with the angle of attack

$$n_{\alpha} = \frac{dn}{d\alpha} = \frac{1}{m \cdot g} \cdot \frac{dL}{d\alpha} = \frac{\frac{1}{2} \rho v^2 \cdot C_{L\alpha}}{g \cdot \left( \frac{m}{S_W} \right)} \quad (7.36)$$

Consequently the smaller the wing loading, the more intensely the aircraft reacts to the vertical gust.

The **tank volume** is proportional to  $S_W^{1.5}$ . This is demonstrated by equation (7.35).

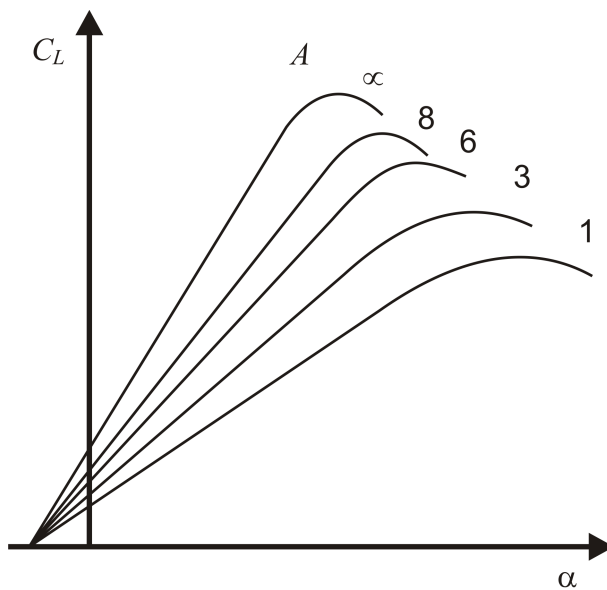
### Wing aspect ratio

The wing aspect ratio  $A = b^2 / S$  has an impact on various parameters:

- A high aspect ratio reduces the **induced drag**  $C_L^2 / (\pi \cdot A \cdot e)$ .
- The **wing mass** of wings with a high aspect ratio is greater than that of wings with a small aspect ratio.
- With an equal wing area, a wing with a higher aspect ratio also has a bigger **span** pursuant to  $b = \sqrt{A \cdot S}$ .
- The smaller the aspect ratio, the smaller the **lift curve slope (Fig. 7.20)**. However, this means that visibility from the cockpit during approach is reduced due to an increased pitch attitude angle. According to equation (7.36), the greater the lift curve slope, and therefore the greater the aspect ratio, the more the aircraft reacts to a vertical gust. In addition, a larger angle for rotating the aircraft at take-off is required.
- The tank volume is proportional to  $\frac{1}{\sqrt{A}}$ . As the aspect ratio increases, the tank volume therefore decreases. This is demonstrated by equation (7.35).

**Table 7.2** Summary evaluation of wing aspect ratio  $A$ 

	Large aspect ratio	Small aspect ratio
<b>Induced drag</b>	small	large
<b>Lift-to-drag ratio <math>L/D</math></b>	large	small
<b>Lift curve slope</b>	large	small
<b>Pitch attitude angle during approach</b>	small (i.e. good visibility from the cockpit)	large (i.e. poor visibility from the cockpit)
<b>Flight in turbulent air</b>	bumpy	smooth
<b>Required angle for rotation</b>	small	large
<b>Wing mass</b>	large	small
<b>Tank volume</b>	small	large
<b>Span (for <math>S_W = \text{const}</math>)</b>	large	small

**Fig. 7.20**

Effect of aspect ratio on the lift curve slope

## Sweep

As explained above, the **critical Mach number** is increased by the sweep. It is irrelevant whether this occurs with the aid of forward sweep or aft sweep.

As a rule, the **maximum lift coefficient** of the wing is reduced due to sweep. The following applies: <sup>2</sup>

$$C_{L,max,swept} = C_{L,max,unswept} \cdot \cos\phi \quad (7.37)$$

<sup>2</sup> Section 8 contains a more precise method for calculating the maximum lift coefficient of swept wings, taking into account the shape of the airfoil leading edge.

This relationship applies approximately to the normally used airfoils with a less sharply defined leading edge. If the wing area is sized by  $C_{L,max}$ , then a larger wing area must be chosen in the case of a larger sweep angle. The **mass of the wing** increases due to the sweep.

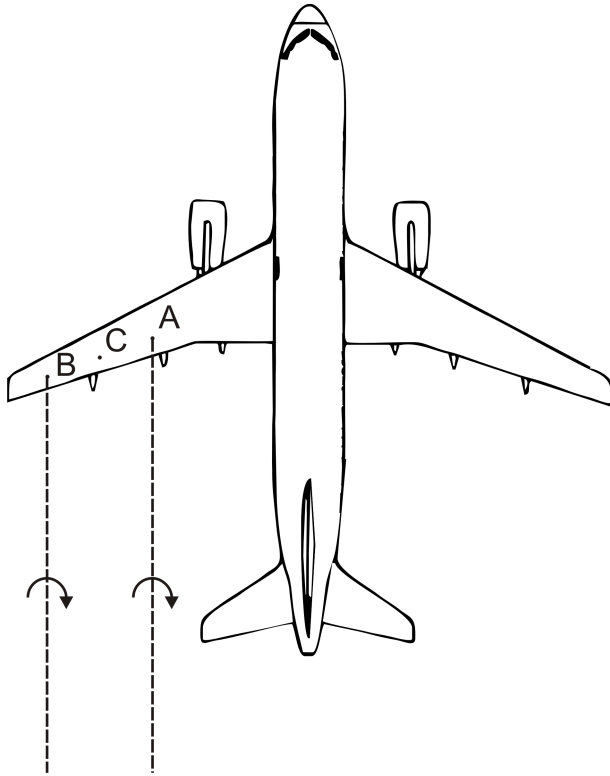
As a rule, the angle of attack of the forward swept wing increases due to the deflection with increasing load. The load increases further due to the increased angle of attack. This positive feed back affecting the forward swept wing leads to divergent behavior. The divergence can be counteracted by an especially stiff wing. However, the necessary additional stiffening increases the wing mass. Consequently **forward swept wings are heavier than aft swept wings**.

The **stall behavior** of forward swept wings is considerably better than that of aft swept wings. The aim is to stall the inner wing first and then the outer wing. In this way, the outer aileron remains effective in the stalled state, so that one-sided “tipping” of the aircraft over one wing can be prevented. **Fig. 7.21** and **Fig. 7.22** explain why a forward swept wing has better lift distribution for the stall behavior. In the case of the aft swept wing, the flow separates first at the wing tip (**tip stall**). This undesirable behavior is also exacerbated by the fact that the boundary layer moves outward with the flow. In older aircraft an attempt was made to keep the inner wing's boundary layer in place on the inner wing with the aid of stall fences (**Fig. 7.23**).

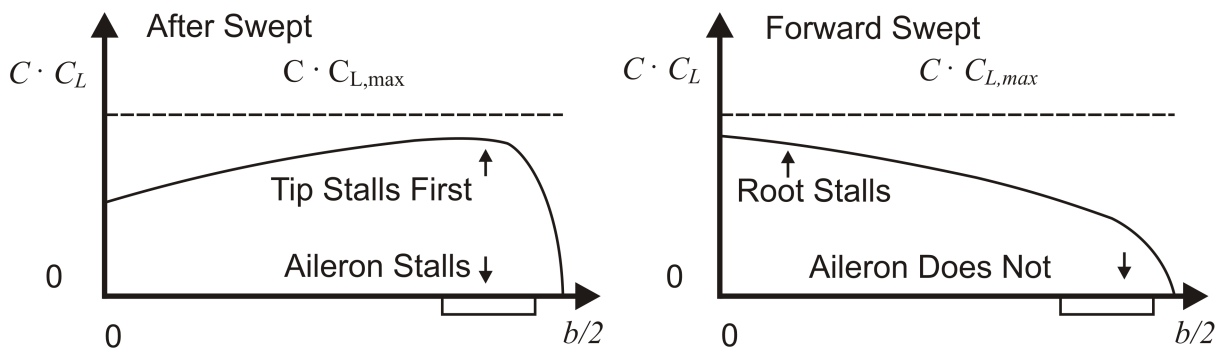
An additional problem associated with tip stall is the change in the pitching moment. As the wing tips are behind the center of gravity in the case of the aft swept wing, the tip stall results in a nose up moment and **pitch up** of the aircraft. If the pilot does not counteract this immediately, the aircraft will stall even more.

The main landing gear and the wing are approximately located at the center of gravity of the aircraft. In the case of swept wings the mean aerodynamic chord is approximately at the center of gravity, but not the wing root. Swept wings therefore cause problems with the **installation of landing gear**. An additional area on the double tapered wing  $S_3$  according to Fig. 7.4 and Fig. 7.5 may solve the problem.

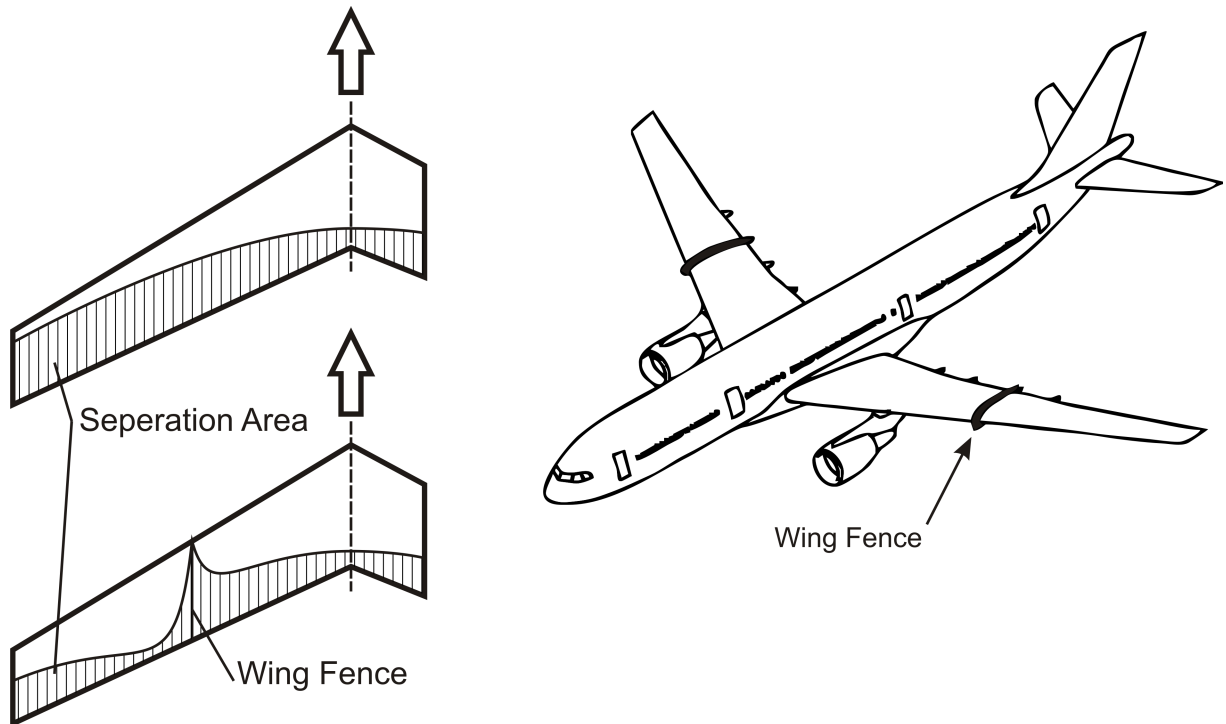
Equation (7.24) shows that the **lift curve slope** decreases as the sweep increases. Thus, the flying characteristics improve in gusty weather, but visibility from the cockpit is worse during the approach due to an increased pitch attitude angle. A larger angle is required at take-off for rotating the aircraft.

**Fig. 7.21**

A filament of flow emanating from Point A has a greater influence on Point C than the influence traveling back from Point B to C. Therefore Point C experiences a greater downwash overall than would be the case for a wing without sweep. The effect thus described results in a lift distribution on the aft swept wing, as shown in Fig. 7.22 (left). In the forward swept wing, the argumentation applies accordingly and leads to the lift distribution in Fig. 7.22 (right)

**Fig. 7.22**

Influence of the sweep on the lift distribution and the stall behavior. The reason for the differing lift distribution is explained by Fig. 7.21

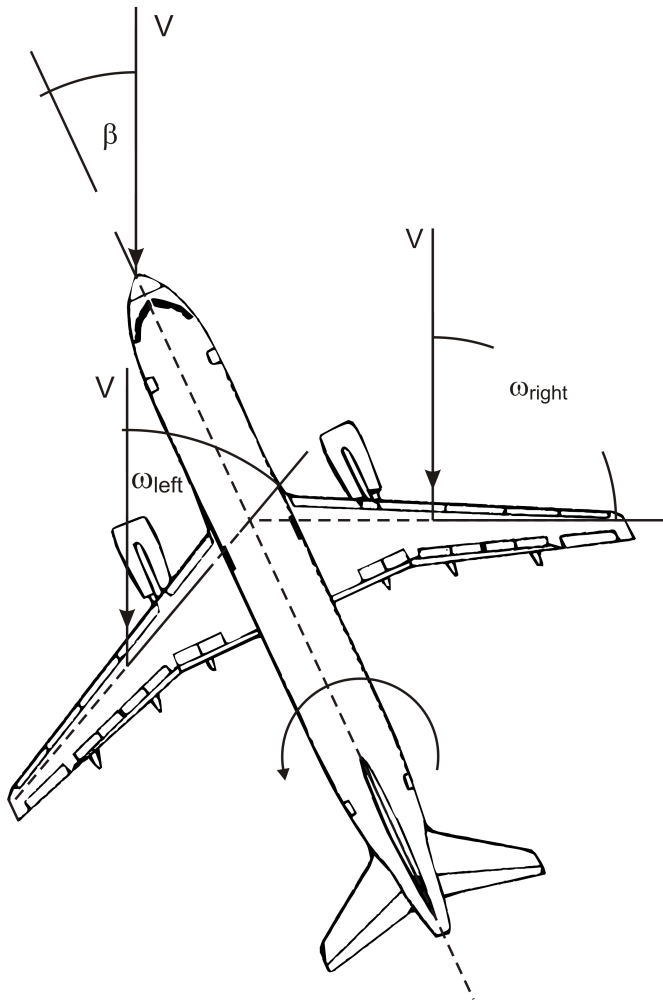


**Fig. 7.23** High angles of attack lead to separation of the flow, usually beginning at the trailing edge. An aft swept wing has a larger area of separated flow at the outer wing than at the inner wing. A stall fence is used in an attempt to positively influence the boundary layer and the separation zone at the outer wing

Aft swept wings exhibit positive **stability around the longitudinal axis**. This is explained with help of (Fig. 7.24) the effect is based on  $C_{L,max,swept} = C_{L,max,unswept} \cdot \cos\phi$  as given in (7.37). If we assume a positive side slip angle (as drawn in Fig. 7.24)  $\omega_{right} > \omega_{left}$  and hence  $C_{L,right} > C_{L,left}$ . This causes a rolling moment to the left.

Aft swept wings however exhibit a destabilizing effect on the **Dutch roll**. The aircraft may need an electronic yaw damper to cope with this problem.

Forward swept wings are basically unstable around the longitudinal axis and therefore require a positive dihedral angle to compensate. The dihedral effect is examined in more detail in the subsection on the dihedral.

**Fig. 7.24**

Positive stability around the longitudinal axis by means of aft swept wings

The **appearance of an aircraft** should not be underestimated. According to general opinion, a swept wing looks better, and what looks good also sells better. This all the more true in the case of private aircraft and business jets. However, experience has shown that tastes tend to be conservative. Designs which are too futuristic might experience problems on the market.

**Table 7.3** Summary evaluation of wing sweep  $\phi_{25}$ 

	Large sweep	Small sweep
<b>Critical Mach number</b>	large	small
<b>Maximum lift coefficient</b>	small	large
<b>Lift curve slope</b>	small	large
<b>Pitch attitude angle during approach</b>	large (i.e. poor visibility from the cockpit)	small (i.e. good visibility from the cockpit)
<b>Flight in turbulent air</b>	smooth	bumpy
<b>Required angle for rotation</b>	large	small
<b>Integration of landing gear</b>	difficult	minor problems
<b>Wing mass</b>	large	small

**Table 7.4** Summary evaluation of type of wing sweep

	<b>Forward sweep</b>	<b>No sweep</b>	<b>Aft sweep</b>
<b>Risk: tip stall</b>	none	none	large
<b>Risk: pitch up</b>	minor	none	large
<b>Maximum lift coefficient</b>	small	large	very small
<b>Risk: one-sided stall</b>	minor	very minor	large
<b>Risk: divergent wing deflection</b>	yes	no	no
<b>Wing mass</b>	very large	small	large
<b>Stability around the longitudinal axis</b>	unstable (requires dihedral for stability)	neutral	stable

**Variable sweep** is chosen for the following reasons:

- good take-off and landing characteristics,
- minimal drag and good flying characteristics in cruise flight,
- optimum lift-to-drag ratio in all flying ranges.

Variable sweep has the following drawbacks:

- the structure of the pivoting mechanism is heavy and expensive,
- the drive system of the variable swept wing is heavy and expensive
- changing the sweep angle causes considerable shifts in the aerodynamic center; large empennages are required to compensate for the resulting moments.

### Relative thickness

- **Drag.** Large airfoil thickness causes a high profile drag<sup>3</sup> in the subsonic range. It also causes high wave drag at transonic and supersonic speed. In the case of supersonic speed, the wave drag is proportional to  $(t/c)^2$ . This explains why supersonic aircraft require extremely thin wings.
- Large relative thickness reduces the **wing mass** because both the bending stiffness and the torsional stiffness are increased.
- The **maximum lift coefficient** rises as the relative thickness increases. This applies up to a relative thickness of approximately 12% to 14%.
- The **volume of the fuel tank** in the wing increases in proportion to the relative thickness. This is shown in equation (7.35).

Conclusion: The relative thickness should always be as large as possible while still being compatible with drag requirements.

<sup>3</sup> Profile drag = frictional drag + form drag

**Table 7.5** Summary evaluation on relative thickness

	Small relative thickness	Large relative thickness
<b>Maximum lift coefficient</b>	small	large
<b>Lift curve slope</b> Equation (7.24)	small	large
<b>Drag</b>	small	large
<b>Tank volume</b>	small	large
<b>Wing mass</b>	large	small

## Taper ratio

The taper ratio  $\lambda = c_t / c_r$  has an influence on the **lift distribution** in the direction of the span. Lift distribution means the graphical representation (**Fig. 7.25**) of the function  $c \cdot c_L$  over the dimensionless distance from the plane of symmetry in the direction of the span  $y / (b / 2)$ . The smallest induced drag is obtained for an elliptical lift distribution. This elliptical lift distribution is achieved if all the airfoils are geometrically similar and all chords lines are parallel, and the wing also has an elliptical chord distribution over the span. The lift coefficient (which is calculated by dividing the value  $c \cdot c_L$  by  $c$ ) is *constant* over the span in this case.

Important: 1.) The *lift distribution* (Fig. 7.25)  $c \cdot c_L$  in the direction of the span  $y / (b / 2)$  must be carefully distinguished from 2.) the *distribution of the lift coefficient* (Fig. 7.26)  $c_L$  in the direction of the span  $y / (b / 2)$ . 1) refers to the aerodynamic quality, and 2) refers to the stall behavior of the wing.

The lift distribution on a **rectangular wing** is too “thick” due to the larger chord at the wing tip. The result is roughly 7% higher induced drag. For an unswept wing, the elliptical lift distribution can be approximately achieved by a **tapered wing** with  $\lambda = 0.45$ . The induced drag is then less than 1% higher than the induced drag of the wing with the elliptical lift distribution.

The position of the center of pressure of a wing section moves to the wing root as the taper ratio decreases. The root bending moment (caused by the lift) decreases accordingly. As the thickness of the wing root becomes larger at the same time, a wing with small  $\lambda$  can achieve a smaller **wing mass** than a rectangular wing.

The necessary thickness at the wing tip constitutes a lower limit for the taper ratio  $\lambda$ , as sufficient **installation space** must be available to accommodate ailerons and the relevant mechanisms in the wing.



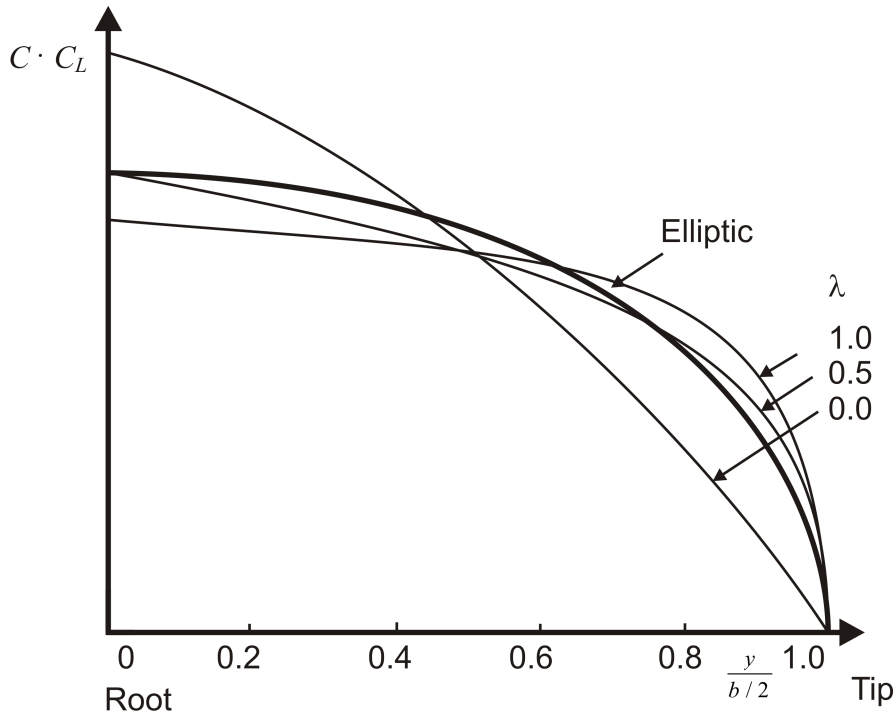


**Fig. 7.25** Lift distribution for various taper ratios at  $\phi = 0$

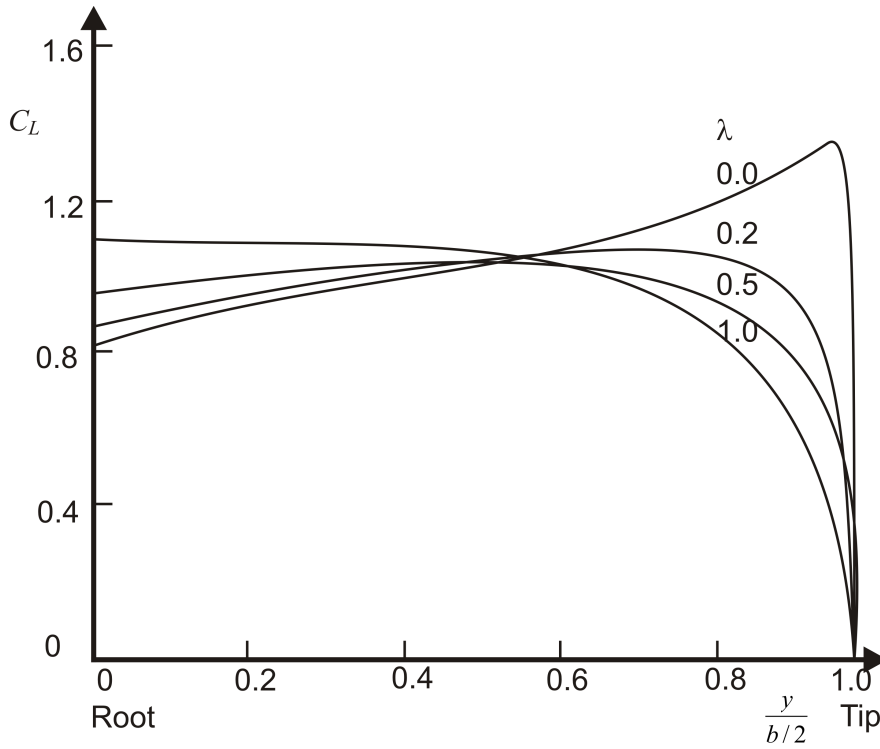


**Fig. 7.26** Distribution of the lift coefficient for various taper ratios at  $\phi = 0$  and aspect ratio  $A = 10$  on a wing with  $C_L = 1$

The taper ratio is an important parameter for controlling **stall behavior**. The lift coefficient distribution in the direction of the span (**Fig. 7.26**) is helpful for the assessment. The flow will separate from the wing first at the point where the lift coefficient distribution reaches its maximum level. To a first approximation the following applies:

$$\text{(only) for } \varphi = 0 : \quad c_{L,max} \text{ is at: } \eta = y / (b/2) = 1 - \lambda \quad . \quad (7.38)$$

With a taper ratio of 0.45, for example, one would consequently expect the flow separation to start at  $\eta = 0.55$ . This is close to the inner end of the aileron and leaves the aileron largely in attached flow. At the same time with a tapered wing with  $\lambda = 0.45$  one also obtains the best approximation for the elliptical lift distribution.

Wings with a positive **sweep** tend to have a “thicker” lift distribution in the vicinity of the wing tip (see above). In order to get close to the elliptical lift distribution again,  $\lambda$  must have smaller values. The optimum taper ratio for the smallest induced drag according to **Torenbeek 1988** can be estimated from the following to a first approximation:

$$\lambda_{opt} = 0.45 \cdot e^{-0.036\varphi^{25}} \quad . \quad (7.39)$$

In equation (7.39) the sweep angle is entered in degrees.  $e$  is the Euler number.

$\lambda$  smaller than 0.2 should be avoided because the short chord at the wing tip can only have small Reynold number. This results in small maximum lift coefficients and **tip stall**. Also the distribution of the lift coefficient (Fig. 7.26) shows a danger of tip stall in the case of small  $\lambda$  values.

It can be ascertained from equation (7.35) that for wings with a constant relative thickness over the span, a taper ratio of  $\lambda = 0$  (triangular wing) offers the largest **tank volume**.

Rectangular wings ( $\lambda = 1$ ) can be manufactured with minimal **production costs**.

Commercial jet transports use double tapered wings, as shown in Fig. 7.5. The additional area S2 is called a “glove”, and area S3 is called “yehudi”. The benefits are:

- an increase in the thickness at the wing root,
- a reduction in the relative thickness at the wing root in order to achieve higher drag divergence Mach numbers  $M_{DD}$ ,
- increase in the sweep (by means of the glove) in order to achieve higher drag divergence Mach numbers,
- increase in the installation space for the landing gear (by means of “yehudi”),

- reduction in the sweep of the inner flaps (by means of “yehudi”) in order to achieve a larger maximum lift coefficient.

**Table 7.6:** Summary evaluation with regard to taper ratio

	Taper ratio $\lambda$ small	Taper ratio $\lambda$ large
<b>Tip stall</b>	bad	good
<b>Tank volume at t/c = const</b>	large (optimum for $\lambda = 0$ )	small
<b>Production costs</b>	-	advantage only for $\lambda = 1$
<b>Installation space for aileron</b>	small	large
<b>Wing mass</b>	small	large
<b>Induced drag in the case of large sweep</b>	small	large

## Twist

The twist is defined as

$$\varepsilon_t = i_{w,tip} - i_{w,root} . \quad (7.40)$$

Many wings are built with negative wing twist  $\varepsilon_t$ , so that the incidence angle  $i_w$  decreases in the direction of the wing tip (Fig. 7.8). This measure is used to **prevent tip stall**. Especially aft swept wings must be given negative twist in order to prevent tip stall.

Twist helps to achieve an elliptical **lift distribution**. However, it is only possible to achieve this with *one* lift coefficient. With other lift coefficients, reduced lift-to-drag ratios are produced, compared to the elliptical lift distribution. If the twist is limited to  $5^\circ$ , these losses can be kept to a minimum. Wash out reduces the root bending moment. Thus the **wing mass** can be reduced. In preliminary design the following can be applied if no other data is given:

$\varepsilon_t = -3^\circ$  (wash out). However the A310 (see Subsection 7.5) shows  $\varepsilon_t = -8^\circ$ .

## Dihedral

Dihedral may occur as a positive dihedral angle, as shown in Fig. 7.6, or as a negative dihedral angle (anhedral). In sideslip, a positive dihedral angle causes a **moment around the longitudinal axis**, which causes the wings to level. A positive dihedral angle therefore leads to positive stability around the longitudinal axis. **Fig. 7.27** shows how the flow acts on a wing with a dihedral: The aircraft flies with its left wing down. This causes the aircraft to slip to the left. The side slip velocity  $V$  approaches the wing from the left. Due to dihedral this causes a difference in the angle of attack on wing section 1 respectively 2. On section 1 lift is increased whereas on section 2 lift is decreased. The resultant moment causes the wing to level again. The wing leveling moment increases with dihedral angle:

$$\Delta \alpha_1 = \frac{V_n}{U}$$

$$\beta = \frac{V}{U} \quad \text{and} \quad V_n = V v_w$$

$$\text{hence} \quad \Delta \alpha_1 = \beta v_w .$$

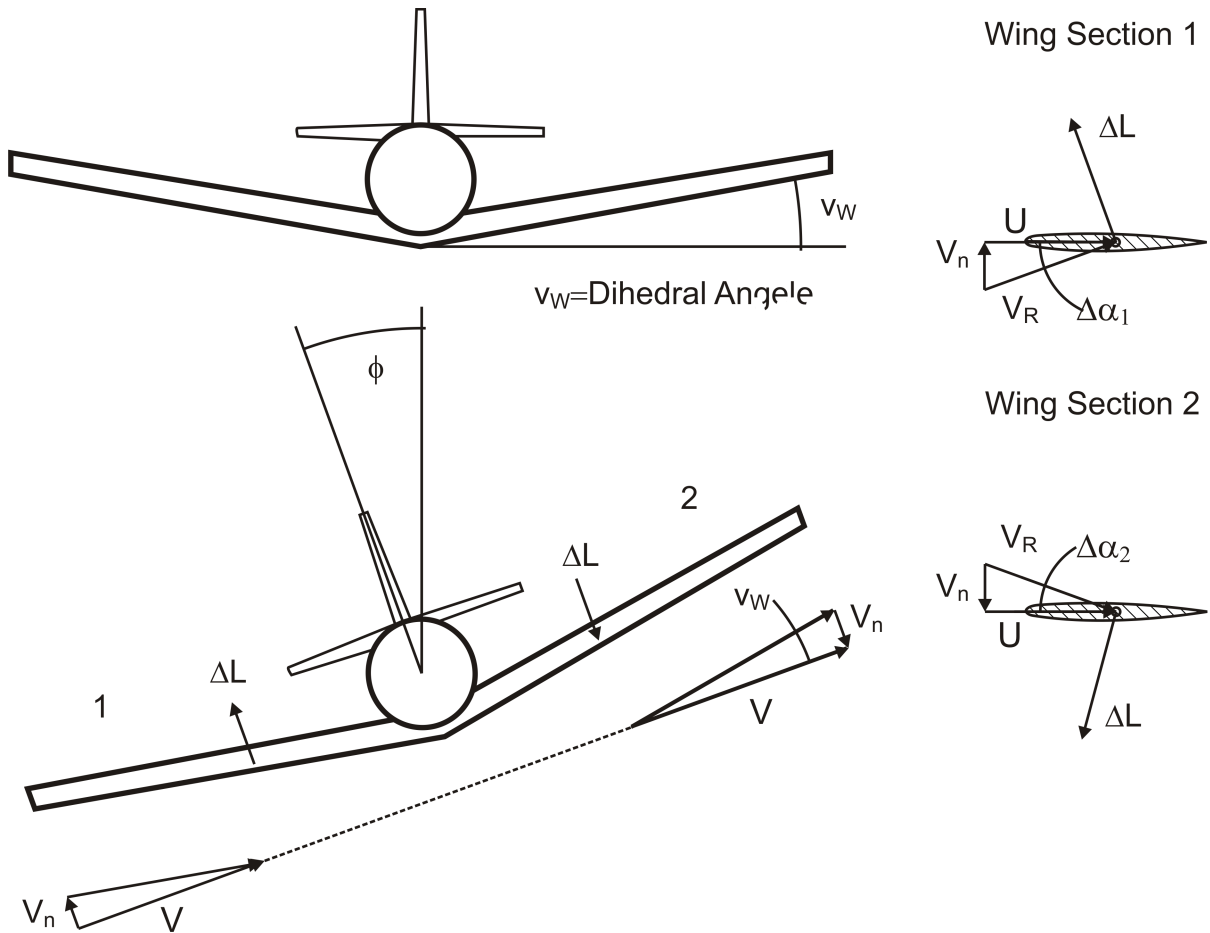


**Fig. 7.27** The flow on the wing with a positive dihedral leads to a moment around the longitudinal axis that causes the wings to level.  
 $V$  velocity due to sideslip  
 $V_n$  normal component of side velocity  
 $U$  forward velocity  
 $V_R$  resultant velocity

The moment around the longitudinal axis in sideslip leads to

- a stable **spiral mode**,
- an unstable **Dutch roll**.

A stabilizing moment around the longitudinal axis in sideslip is achieved by

- a positive dihedral angle,
- a wing configuration in relation to the fuselage in the form of a high-wing aircraft,
- an aft swept wing.

A destabilizing moment around the longitudinal axis in sideslip is achieved by

- a negative dihedral angle (anhedral),
- a wing configuration in relation to the fuselage in the form of a low-wing aircraft,
- forward swept wing.

10° sweep achieves roughly as much as 1° dihedral.

Moving the wing position in relation to the fuselage by “one step”  
(e.g. from high to middle, or from middle to low)  
achieves roughly as much as 3.5° dihedral

The combination of aft sweep and high-wing configuration together achieve so much stability that it has to be counteracted with an anhedral. For example, Avro RJ85 (see Section 4).

**Table 7.7** Instructions for choice of dihedral

Dihedral angle in °	Low wing	Mid wing	High wing
<b>Unswapt wing</b>	5 to 7	2 to 4	0 to 2
<b>Swept wing</b>	3 to 7	-2 to 2	-5 to -2

Dihedral is also used to ensure the necessary **clearance of engines and wing tips from the ground**.

## Incidence angle

The incidence angle  $i_w$  is defined in Fig. 7.7.

The incidence angle should be chosen so as to ensure that the **drag in cruise flight** is as low as possible. For this, the fuselage longitudinal axis should be parallel to the direction of the flow. In case of doubt, the fuselage can have a small positive incidence angle in cruise flight. However, if the incidence angle is negative, the fuselage produces negative lift and therefore additional drag.

The incidence angle should be chosen so that the **cabin floor is horizontal in cruise flight**. If the cabin floor diverges too much from the horizontal, it can become difficult for the cabin crew to push the trolleys through the aisles. Furthermore, servicing in a passenger aircraft should start already towards the end of the climb. Labor unions define which floor angle is ac-

ceptable for the crews during servicing. On the basis of the requirement of a horizontal fuselage in cruise, the incidence angle can be estimated (**Roskam III**):

$$i_w = \frac{C_{L,CR}}{C_{L\alpha}} + \alpha_0 - 0.4 \cdot \varepsilon_t . \quad (7.41)$$

In this equation:

- $C_{L\alpha}$  the lift curve slope according to equation (7.24),
- $C_{L,CR}$  the necessary lift coefficient in cruise flight,
- $\alpha_0$  the angle of attack at zero wing lift or a characteristic profile of the wing,
- $\varepsilon_t$  the twist (see above).

The factor 0.4 tries to account for the fact that we have a tapered wing with the inboard wing having more area and hence more contribution towards overall lift than the outboard wing.

It must be borne in mind

- that  $\alpha_0$  and  $\varepsilon_t$  are negative, as a rule.
- that  $C_{L\alpha}$  from equation (7.24) is obtained in radian (rad) and has to be converted into degrees ( $^\circ$ ) for equation (7.40) if  $\alpha_0$  and  $\varepsilon_t$  are also in degrees.

If the incidence angle is too small, **visibility from the cockpit** onto the runway may no longer fulfill the requirement in the **landing approach**.

If the incidence angle is too great, the **nose wheel** may touch down first during **landing**. This must always be avoided, as the nose landing gear is not designed to absorb landing impact. It is only possible to determine whether such a risk exists after defining the high lift system. In this respect, it is critical if only flaps, but no slats, are envisaged for an aircraft. In this case, the aircraft will reduce its pitch attitude angle during landing approach after extending the flaps.

## Summary of key characteristics

Table 7.8 contains a summary of key characteristics of wing design parameters.

Table. 7.8 Summary of key characteristics of wing design parameters based on Schmitt 1998

effect of an increase off → on ↓	$S_w$	$A$	$\phi$	$\lambda$	$t/c$
low speed flight	+++ lifting capacity	+++ 2. segment	- $C_{L\max}$	++ depending on plan view	++ $C_{L\max}$
high speed flight	++ aerodyn. quality buffeting $M_{Dive}$	++ aerodyn. quality	++ $M_{Dive}$	-	-- $M_D$
wing mass $m_w$ low => +	- big wing => heavy	--- $h_{Wingbox}$ bending moment	-- bending moment	- $h_{Wingbox}$	+++ $h_{Wingbox}$
fuel tank $V_F$ high => +	++ $\sim S^{1.5}$	- $\frac{1}{\sqrt{A}}$	$\approx 0$	$\frac{1 + \lambda + \lambda^2}{(1 + \lambda)^2}$	+++ $\sim t/c$
wing stiffness	++ $h_{Wingbox}$	-- $h_{Wingbox}/b$	-- $b_{50\%}$	- $h_{Wingbox}$	+++ $h_{Wingbox}$

## 7.4 Ailerons and Spoilers

Most aircraft use ailerons and/or spoilers for rolling. In doing so, the large lever arm of the wings can be utilized. Some fighter aircraft create an (additional) roll moment through the asymmetrical deflection of the elevator.

The yawing movement initiated by the vertical rudder also leads to rolling (due to a positive yaw/roll moment). However, this coupling is so weak that no satisfactory maneuverability can be achieved around the longitudinal axis in normal operation with the rudder alone.

### Ailerons

Ailerons are simple plain flaps that are normally mounted close to the left and right wing tips. The position of the ailerons enables a large lever arm to be utilized. The ailerons on both wing tips deflect in opposite directions.

Ailerons cause an **adverse yaw**. This adverse yaw causes the aircraft to first yaw in a direction that is contrary to the initiated turn. The adverse yaw has to be compensated for with the rudder, and can be reduced if the ailerons are designed so as to deflect further upward than down-

ward. A special aileron geometry, which also serves to reduce the adverse yaw, is shown in **Fig 7.28**.

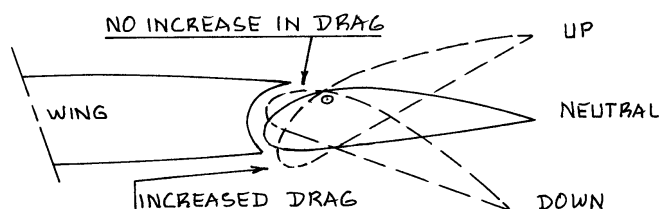


**Fig. 7.28**

Aileron with special geometry to reduce the adverse yaw (**Roskam III**)

The deflection of an aileron on a wing tip (outer aileron) can twist the wing so such an extent that the aircraft performs a roll movement that is contrary to what was initially intended by the aileron deflection. The phenomenon is called **aileron reversal** and can occur in the case of high dynamic pressures and wings with low torsional rigidity. In such cases, the aileron must be fixed when high dynamic pressures occur. Roll movements are then initiated with spoilers – or with ailerons that are mounted further inboard on the wing (inner aileron).

It is important to bear in mind that ailerons “compete” with flaps for the space on the trailing edge. The high lift system can be especially effective if the entire span is available for flaps. The problem can be solved in some cases by deflecting the ailerons downward symmetrically together with the flaps, e.g. 20% of their full deflection (**aileron droop**), so that they support the high lift system. However possibilities for aileron droop are limited because flaps are used in low speed flight and this is exactly the situation when high aileron deflections are needed. Thus aileron droop may not cause aileron efficiency to be reduced too much.

When choosing the geometry of the ailerons, the geometry of completed aircraft can be used as a guide in the preliminary design. The chord of the ailerons is normally **20% to 40% of the wing chord**. Typical values are roughly 30% of the wing chord. Ailerons are normally in the region of 40% to 100% of the semi-span. Typical ailerons cover **65% to 95% of the semi-span**.

## Spoilers

Spoilers do what their name says, i.e. they “spoil” the flow over the part of the wing that is located directly behind the spoilers. **Fig. 7.29** shows the effect. Spoilers are very effective with extended flaps. In contrast to ailerons, spoilers do not cause adverse yaw, but rather a yawing movement in the direction of the turn being flown. Due to the principle on which spoilers function, drag is also produced by spoiler deflection. Therefore, the flight control sys-



tem is often designed so that the ailerons are used first and the spoilers are only employed when higher roll rates are required.

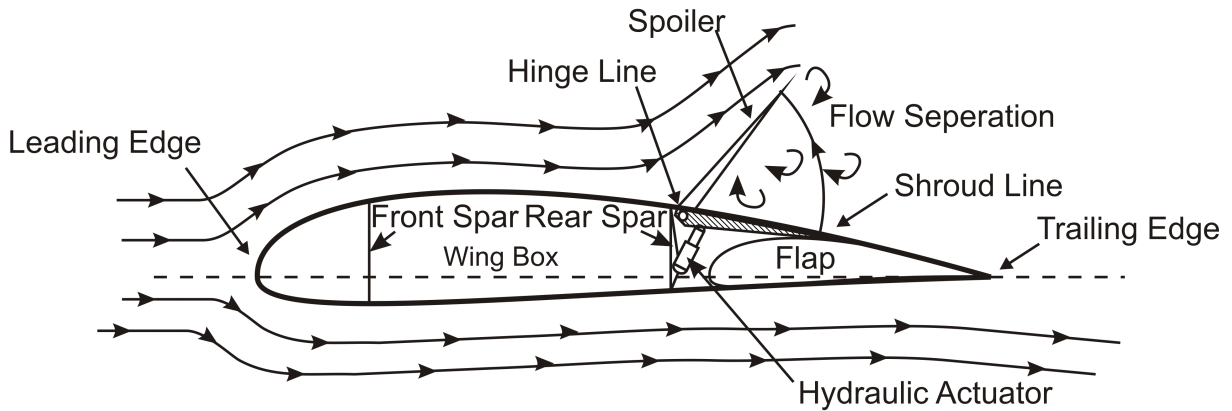


**Fig. 7.29** Arrangement of a spoiler on a wing section

Spoiler geometries can be found in “Jane's all the World's Aircraft” (**Lambert 1993**). The three-views from Section 4 can also be used to gain an initial impression of spoiler geometries.

Most aircraft use a **wing box** to absorb forces and moments. The front and rear limits of the wing box are defined by the front and rear spars. The **location of the spars** must be chosen so as to be **compatible with the high lift system** and the **control surfaces**. As can be seen in Fig. 7.29, the hinge line of the spoilers is located directly behind the rear spar. Space has to be left between the rear spar and the hinge line to accommodate the drive mechanism of the ailerons. **Typical locations for the spars** are as follows:

- Front spar: 15% to 30% of the chord,
- Rear spar: 65% to 75% of the chord.

After deciding where to locate the spars, it is possible to calculate the **volume of the fuel tank** more precisely than was possible with the semi-empirical equation (7.35).

## 7.5 Example: The Wing of the Airbus A310

**Table 7.9** A310 wing characteristics

Reference surface area (Sref) (aerodynamic)	219 m <sup>2</sup>
Aspect ratio (aerodynamic)	8,8
Total wing span (b)	43,90 m
Sweep at 25% MAC (aerodynamic)	27,97 °
Root chord	8,381 m
Kink chord (basic trapezium)	4,946 m
Tip chord	2,175 m
Mean aerodynamic chord (MAC)	5,829 m
Root thickness/chord ratio	15,2 %
Kink thickness/chord ratio	11,8 %
Tip thickness/chord ratio	10,8 %
Inner trailing edge dihedral	11,8°
Outer trailing edge dihedral (Jig shape)	4,3°
Root wing setting	5,3°

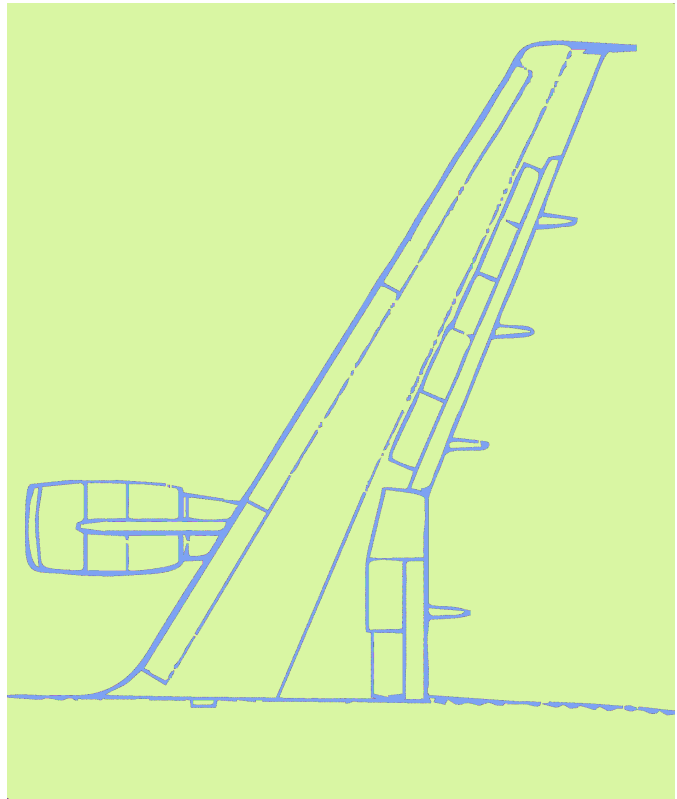


**Fig. 7.30** A310 wing planform

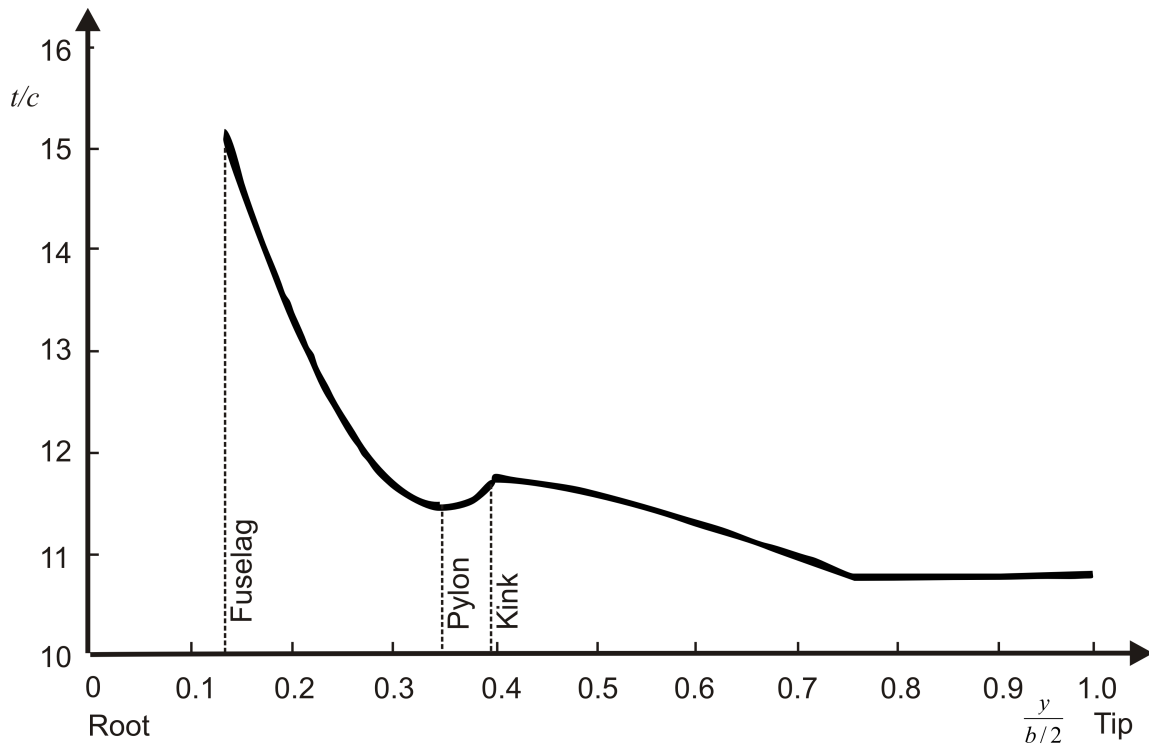


**Fig. 7.31** A310 distribution of relative wing thickness

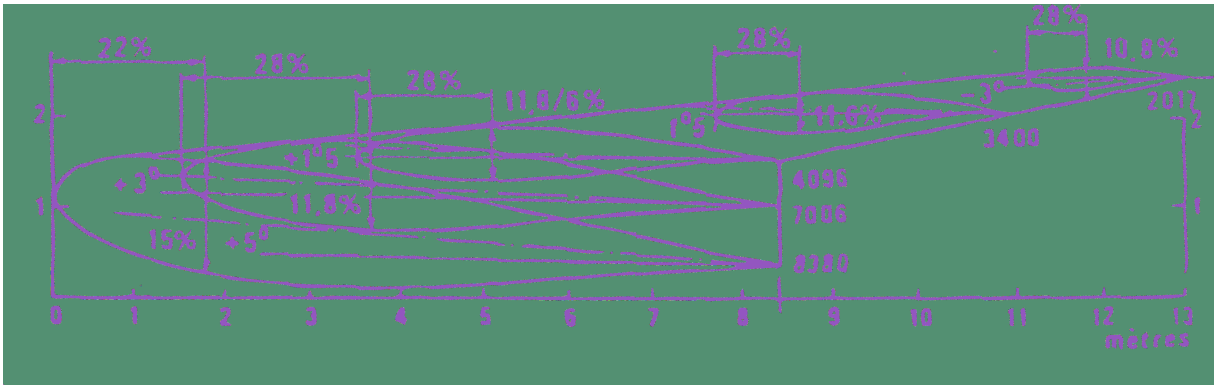


**Fig. 7.32** Airbus A310 wing: sections, chord, relative thickness, wing twist, and incidence angle (quoted from **Obert 1997**)

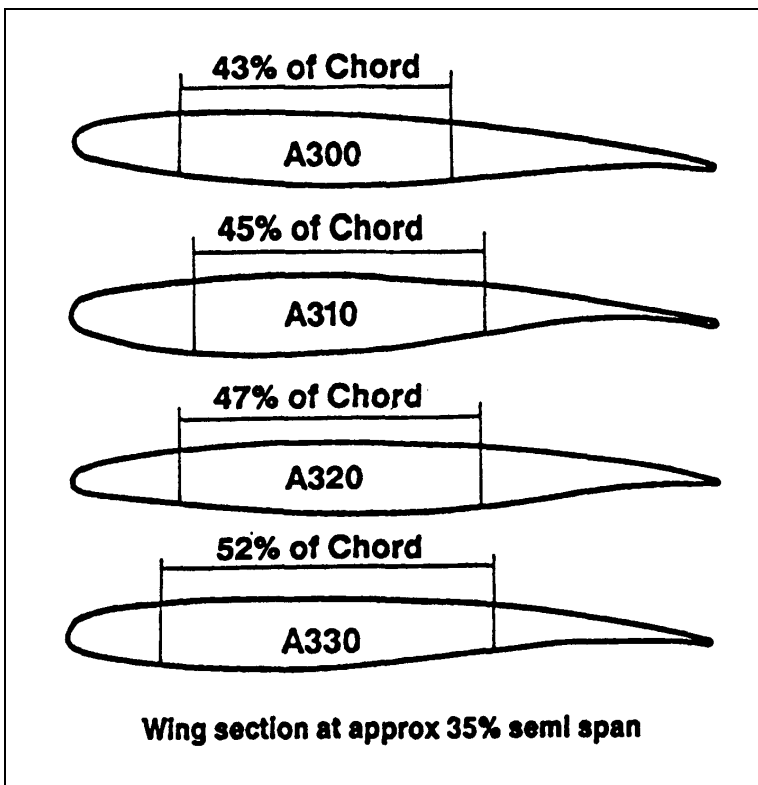


**Fig. 7.33** Wing section and wing box at 35% semi-span of Airbus A310 in comparison with other Airbus aircraft

Acknowledgement: Table 7.9, Fig. 30, Fig. 31, and Fig. 33 are courtesy of Airbus.